**Proteomic Characterization of the Chorion**

by

**Jennifer Downing Scholler**

B.S., University of Wisconsin – Madison, 2007

A thesis submitted to the

Faculty of the Graduate School of the

University of Colorado in partial fulfillment

of the requirements for the degree of

Master of Science

Department of Mechanical Engineering

2012

This thesis entitled:
Proteomic Characterization of the Chorion
written by Jennifer Downing Scholler
has been approved for the Department of Mechanical Engineering

Virginia Ferguson, PhD

Karen Jonscher, PhD

Date:

The final copy of this thesis has been examined by the signatories, and we find that both the content and the form meet acceptable presentation standards of scholarly work in the above mentioned discipline.

IRB Protocol # 06-1159

Scholler, Jennifer D. (M.S., Mechanical Engineering – Bioengineering)

Proteomic Characterization of the Chorion

Thesis directed by Professor Virginia L. Ferguson, PhD

**Abstract**

The complex mechanisms behind membrane rupture remain poorly understood, presenting a problem for clinicians attempting to predict and prevent preterm births. In particular, there is a lack of information in the literature about the protein content of the chorion. This thesis establishes a characterization of the protein content of the chorionic layer of the fetal membranes and examines differing protein content across different regions of the membranes (proximal to and distal from the rupture site) and between membranes with differing modes of rupture (spontaneous versus artificial). A more thorough understanding of membrane rupture in both term and preterm cases is required to improve diagnostic methods and prevent PPROM.

Fetal membranes were collected from term, vaginal deliveries with no known pregnancy-related complications. Samples were collected from spontaneously rupturing (SROM; n=5) and artificially rupturing (AROM; n=2) membranes. For each membrane, samples were taken proximal to and distal from the rupture initiation site. Mass spectrometry identified several proteins involved in assembly, wound response and immune response as differentially expressed between the placental and rupture regions. In particular, basement membrane proteins including fibrillin and laminin were observed exclusively in the artificially rupturing samples, and fibrinogen was found in the rupture region in AROM but not SROM samples. Talin and vinculin, proteins involved in focal adhesions, were observed exclusively in AROM rupture.

Collagen content was analyzed by hydroxyproline assay. No difference in collagen concentration was observed based on mode of rupture or region. These results were supported by histology. Sulfated

glycosaminoglycan content was quantitated by DMMB assay. Within the placental region, sGAG content was significantly reduced in SROM samples. Within each mode of rupture group, no regional difference in sGAG content was seen, although a pairwise reduction that did not reach significance was observed for the rupture region for most samples. Safranin O stained histology slides appeared to show an increase in proteoglycan content in rupture, which may be due to an increase in the non-sulfated GAG hyaluronan. Finally, a consistent, but not significant, pairwise increase in chorion thickness was seen in the rupture region.

**Acknowledgments**

I would like to thank Dr. Jonscher and Dr. Ferguson for advising me during this project. I'd also like to thank Dr. Wei Tan for serving on my thesis committee. I am further grateful for the advice and assistance of Brandi Briggs, Dr. Blair Dodson and Dr. Kirsten Kinneberg. Veronica Hogg-Cornejo and Carson Petrash were also very helpful in establishing certain protocols and generally assisting in labwork. This project greatly benefitted in terms of clinical advice and assistance in sample preparation from the efforts of Dr. Virginia Winn, Dr. Meghan Donnelly and Anita Kramer. Additionally, I owe thanks for Dr. Miriam Post for her assistance in interpreting histology slides, to Dr. Matt McQueen for his biostatistics advice, and to Joe Gomez for running our samples on the mass spectrometer. Thanks are also owed to several of my classmates who have become friends and supporters, and who helped allay stressful situations and made me look forward to heading to class. Finally, I'd like to thank my husband, Joe, who agreed to move over 1000 miles so that I could achieve my goals.

**Contents**

**List of Tables**

**List of Figures**

## 1. Introduction & Background

Despite many advances in medical technology, preterm birth rates remain high, reaching 12.8% worldwide in 2006 [1]. Preterm premature rupture of the fetal membranes (PPROM) occurs in 3% of pregnancies and is responsible for around one third of all preterm births [2]. PPROM occurs when the membranes rupture prior to 37 weeks gestation and prior to the onset of labor [2]. The etiology of spontaneous membrane rupture and specifically preterm rupture remains poorly understood, causing a problem for clinicians. Preterm birth is associated with significant health complications for the neonate. Respiratory distress syndrome (RDS) is the most common serious complication following PPROM [2]. Other complications include necrotizing enterocolitis, intraventricular hemorrhage, and sepsis [2]. Studies so far have failed to find a singular cause for PPROM, indicating that its causes are likely multifactorial [3]. Although the exact causes of membrane rupture are unknown, the maintenance of membrane tensile strength requires an equilibrium between the synthesis and degradation of the proteins within the extracellular matrix (ECM) [3]. The physical and biological properties (including strength and propensity to degradation) of the ECM are greatly affected by changes in the content and composition of the ECM [4]. ECM composition in the fetal membranes is at least partly controlled by matrix degrading enzymes, particularly the matrix metalloproteinases (MMPs) [4]. The role of MMPs in membrane rupture is discussed in-depth in a following section. The ECM components contain cryptic matrikines that can be exposed by conformational change or proteolysis and then can stimulate the production of cytokines and MMPs [4], contributing to degradation and rupture.

In some studies, a decrease in collagen content was seen in PPROM [5]. Amnion levels of mRNAs of some of the procollagens and enzymes required for collagen synthesis (prolyl 4-hydroxylase and lysyl hydroxylase) are highest in early gestation and drop off between 12 and 14 weeks [4], indicating that

reduction in collagen may play a role in readying membranes for spontaneous rupture in normal term pregnancies.

The coupling of mechanical and biochemical changes likely contribute to both normal and preterm rupture. Physical forces such as stretch may initiate biochemical responses causing changes in the supracervical portion of the membranes [6], resulting in rupture. It is hypothesized that fetal membrane rupture starts with distension and loss of elasticity, followed by separation of the chorioamnion, 'disruption of the chorion', 'distension', 'herniation of the amnion', and finally amnion rupture [7]. Increased separation of the chorioamnion has also been seen with both increasing gestational age and labor [7], [8], [9]. Apoptosis within the membranes likely also plays a role in rupture, as apoptosis within the chorioamnion has been seen in PPROM and normal term rupture alike [4]. Although some factors contributing to membrane rupture have been identified, a more thorough understanding of its mechanisms is required for improved clinical prevention and treatment of PPROM.

### 1.1. Fetal membrane structure & function

The fetal membranes surround the fetus during gestation and contain the amniotic fluid. They are composed of two layers: the amnion and the chorion. The amnion is the inner (toward the fetus) layer, while the chorion is the outer layer. Together, they are referred to as the fetal membranes or the chorioamnion.

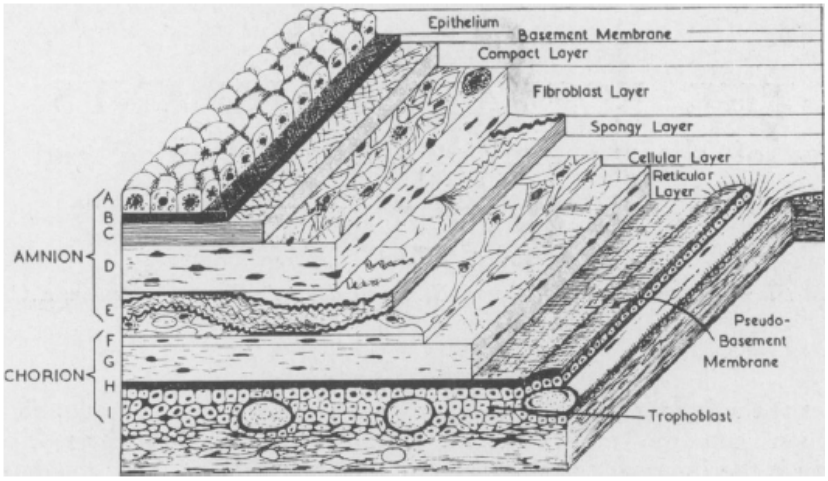


Figure 1: Layers of the chorioamnion.[10]

The amnion is thinner, but has a higher tensile strength. Typically the amnion is between 0.02 and 0.5 cm thick [10]. It consists of five layers:

the epithelium, the basement membrane, the compact layer, the fibroblast layer, and the spongy layer (listed in order from the amniotic cavity toward the chorionic layer) [10]. The layers of the entire chorioamnion can be seen in Figure 1.

The amnion is avascular and without nerves. All the required nutrients are provided to the amnion tissue by the amniotic fluid. The innermost layer of the amnion is the epithelium. The epithelial layer secretes collagen types III and IV and noncollagenous proteins such as laminin, nidogen and fibronectin, which form the basement membrane layer [11]. It also produces MMPs 1, 2, and 9 [11]. The compact layer is a layer of connective tissue composed mainly of collagen types I and III [11]. It forms the main fibrous structure of the amnion and is secreted by cells of the fibroblast layer [11]. Within the compact layer, collagen types V and VI form connections between collagen types III and IV and the basement membrane [11]. The fibroblast layer consists of loose networks of collagen and glycoproteins along with mesenchymal cells and macrophages [11]. It is the thickest layer within the amnion and it secretes MMP-1, MMP-9, and TIMP-1 [11]. The intermediate, or spongy, layer is the outermost layer of the amnion. It is composed of hydrated proteoglycans and glycoproteins [11]. The spongy layer is comprised of a nonfibrillar network of type III collagen and absorbs physical stresses [11]. The overall collagen content of the amnion is quite variable depending on the study, but literature values range from 33-52% [12], and the hydroxyproline content (a measure of collagen) ranges from 42-52.7 μg/mg dry weight [13], [14], [15]. The soluble collagen content of the whole chorioamnion is about 10.5% of dry weight [12]. The elastin content reported in the literature varies widely. Hieber et al. [16] reported the elastin content of intact chorioamnion as 0.08% of fat free weight whereas Jabareen et al. [12] estimated the elastin content as 2.1%. Wilshaw et al. [17]reported the elastin content of fresh amnion to be 36% of the total weight. The collagen and elastin content of the fetal membranes is important,

particularly in comparing membranes with differing characteristics, because these components help determine much of the mechanical behavior of the chorioamnion.

The chorion layer is thicker but weaker in tension. Thickness measurements of both the amnion and the chorion are quite variable and differ between studies due to differing measurement techniques, but the chorion consistently measures approximately four times thicker than the amnion [12]. The reticular layer is adjacent to the to the spongy layer and consists of collagen types I, III, IV, V, and VI along with proteoglycans [11]. Moving outward away from the fetus, the basement membrane is encountered. Collagen type IV, fibronectin, and laminin comprise the basement membranes [11]. The outermost layer of the chorion and the fetal membranes in general is the trophoblast layer. The trophoblast layer faces the maternal decidua, is thick and obviously highly cellular, and is known to produce matrix metalloproteinase 9 (MMP-9) [11]. The overall collagen content of the chorion is about half of that of the amnion, ranging from 12-15%, with a hydroxyproline content of approximately 16-17 μg/mg dry weight [13], [14]. Although the chorion does not provide the majority of the tensile strength of the membranes, it still may be quite important to overall membrane integrity. The chorion may act as a mechanical buffer to the overall membrane, preventing the intact chorioamnion from experiencing degradation as quickly as the amnion itself does [18]. This may be especially important in labored membranes, and if chorion integrity can be maintained it may help prevent PPROM [18]. Additionally, the highly cellular nature of the chorion means that its secretome (the set of proteins secreted by a tissue or cell), could have important implications to membrane rupture. There is experimental evidence of this effect. Treatment with high doses of cytokines did not significantly weaken isolated amnion [19]. However, when the entire chorioamnion underwent the same treatment and the amnion was subsequently separated and tested, weakening was observed [19]. Moreover, weakening was also seen when isolated amnion was placed in culture medium in which choriodecidua had previously been cultured

with cytokines [19]. The importance of the chorion is also supported by the fact that membrane strength is reduced with delamination of the layers [7], [20]. Although not much study has been completed on the isolated chorion, likely because it is the weaker portion of the membranes, it likely plays an important role in the maintenance of membrane integrity through both mechanical and biochemical means.

In order to effectively treat and prevent PPROM, clinicians must first be able to identify pregnancies that are likely to result in PPROM. The current criteria and diagnostic tests have proved less than ideal. Along with choriodecidual infection and inflammation, decreased membrane collagen content, lower socioeconomic status, cigarette smoking, STIs, prior cervical colonization, prior preterm delivery, uterine distention, cervical cerclage, amniocentesis, and vaginal bleeding in pregnancy have been associated with PPROM [2]. These factors may be associated with PPROM through stretch, degradation, inflammation or weakening of protection to bacterial infection [2]. Preterm birth in a previous pregnancy is not a very effective indicator of future risk, however. Women with prior preterm birth at 23-27 weeks have shown a 27.1% risk of preterm birth with subsequent pregnancies [2]. Those women with previous PPROM had a 13.5% risk of preterm birth due to PPROM [2]. Increased fetal fibronectin in the CVF is also used to predict preterm delivery. Increased levels of fetal fibronectin were found in the amniotic fluid and the cervical and/or vaginal fluids of 93.8% of women with preterm membrane rupture [21]. Elevated (defined as above the threshold for being positively identified in the sample) fetal fibronectin was also found in 50.4% of the women with intact membrane and preterm contractions [21]. Additionally, first time mothers with a positive test for CVF fetal fibronectin and a short cervix had a 16.7% risk of preterm birth due to PPROM, and multiparas with prior history, short cervix, and positive test for CVF fetal fibronectin had a 25% risk of PPROM [2]. Clearly, diagnostic tests that are more accurately able to predict

pregnancies that are at risk for PPROM and preterm birth while not incorrectly flagging normal pregnancies as at-risk are critical if PPROM is to be effectively prevented.

### 1.2. Supracervical 'weak zone'

There is ample evidence that a zone of altered morphology and biochemistry develops over the cervix. These changes lead to mechanical weakness within that zone. This zone of altered morphology is characterized by swelling, disruption of the connective tissue, thinning of the trophoblast layer and thinning of the decidua, and it is coincident with the rupture site [4]. McLaren et al. [22] showed an increase in thickness of the connective tissue layer overlying the cervix compared to the midzone (region midway between the rupture site and the placenta) in prelabor samples using histology. Corresponding decreases in the thickness of the cytotrophoblast and decidual layers were also seen. Moreover, the patients with the greatest structural changes based on the histological study also had the highest pro-MMP-9 activity (see section 1.7 'The role of proteases and their inhibitors in PPROM'). El Khwad et al. [23] also confirmed changes in the supracervical zone when they showed increased levels of MMP-9 and decreased TIMP-3 (see section 1.7 'The role of proteases and their inhibitors in PPROM') and increased PARP cleavage within the cervical zone compared to the rest of the membranes. PARP is an enzyme associated with DNA repair and apoptosis. Collectively these changes are indicative of collagen remodeling and apoptosis. The same study showed a significant decrease in strength in a 10-cm zone centered over the cervix when compared to the rest of the fetal membranes. The mean rupture strength within this supracervical zone was only 55% of that of the rest of the membranes. This is in fairly close agreement with another study that showed the rupture strength within the weak zone to be reduced to around 60% of that of the rest of the membranes [4]. A loss of collagen organization was also observed in this region [24]. Other biochemical changes have also been observed. Cervical

amnion showed a 2-fold increase in biglycan and a 50% decrease in decorin [8]. Biglycan and decorin are both proteoglycans. Decorin increases the tensile strength by binding to collagens I and III, while biglycan opposes the effect of decorin, weakening the bonds between decorin and collagen, and ultimately disrupting collagen's organization [8]. Lappas et al. [25] demonstrated that the MAPK/AP-1 pathway may be involved in ECM degradation in the supracervical zone, facilitating it's rupture, by showing that the intensity and/or extent of the immunohistochemical staining of MAPK and AP-1 proteins (ERK, p-ERK, p-JNK, p-p38 MAPK, cFos, JunB , p-cJun) were greater in chorioamnion from the supracervical site as compared to the distal site. The MAPK and AP-1proteins act to regulate the ECM degrading MMP-9 (See section 1.7) [25].

### 1.3. Mechanical properties of the fetal membranes

Effort has been made to determine the mechanical properties of the fetal membranes, both from a general characterization standpoint as well as with the purpose of identifying mechanical property differences of membranes proximal to and distal from the rupture site. The amnion layer is much stronger than the chorion, with biaxial puncture forces of about twice that of the chorion [18]. Also in biaxial puncture tests, the separate layers of the intact chorioamnion failed in two separate events and the failure of the amnion had a preferred direction [26]. Using pooled data from previous studies, Chua et al. [27] consistently found the failure strength of the chorioamnion to be approximately 0.9 MPa. The pooled data included results from four types of mechanical tests: the uniaxial tensile test, the biaxial inflation (burst) test, the biaxial puncture test, and the planar biaxial test. Using only the pooled data that closely approximated a 'normal' delivery, no correlation was found between failure stress or failure tension (failure force divided by initial specimen width) and gestational age [27]. When all rupture modes and gestational ages were included, there was a decrease in failure stress, but not in failure tension, after 32 weeks gestation [27]. However, using a

biaxial puncture test, Oyen et al. [18]showed that increasing gestational age trended with decreasing puncture strength of the chorioamnion and the isolated amnion for both vaginal deliveries and Cesarean sections, although the trend was only statistically significant for labored deliveries. Chorion puncture forces did not trend with gestational age or mode of delivery, indicating that the chorion did not seem to be affected by the chemical and mechanical changes of gestation and delivery in the same manner as the amnion [18]. Additionally, the study found no major mechanical differences between membranes that ruptured spontaneously during labored delivery and those that ruptured prematurely prior to the onset of labor [18]. Preloading the tissues was seen to increase membrane failure stress values, with more cycles and larger preloads resulting in greater increases in strength [18]. Some of these findings confirmed the findings in a previous study in which labored amnion specimens showed reduced biaxial puncture strength, but the weakening effect was not seen in intact chorioamnion or in isolated chorion [26]. The mechanical properties of the membranes likely reflect both the physical stresses imparted on them as well as biochemical changes within them. An understanding of the mechanical properties, the biochemical properties (addressed in this work) and the interplay between the two will be required to fully understand the mechanisms behind membranes rupture and prevent PPROM.

### 1.4. Biochemical characterization studies

The biochemical composition of the pregnancy-related tissues and fluids has been studied to further understand parturition. This includes the fetal membranes, cervicovaginal fluid (CVF), and amniotic fluid (AF). CVF is a convenient fluid for study and would make an ideal diagnostic sample because it can be sampled noninvasively and with minimum risk. However, the comparison of data from various studies shows that the protein content of CVF samples is quite variable [28], which may undercut its value somewhat. Based on the consistent presence of certain proteins across several

studies despite the overall variability, Zegels et al. suggested that the CVF proteome consists of a fixed 'core proteome' and a variable set of proteins which is dependent on physiological and experimental environments [28]. Immune peptides and proteins including defensins (human beta-defensin 2), lactoferrin, immunoglubulins, azurocidin, myeloperoxidase, TLR-7, and IL-6 were identified in normative CVF [28]. The existence of host defense proteins in the vaginal fluid could yield a technique to study preterm birth associated with infection [29]. Endometrial proteins including glycodelin and ribonucleoprotein A were identified in CVF from nonpregnant women [28]. Many of the other proteins identified in CVF from nonpregnant women had a serine protease function, including kallikrein-6/1-/11/13/14, transmembrane serine proteases 11D/11E, leukocyte elastase, and myeloblastin [28]. Other proteases such as cathepsin G, inhibitors of the serine proteases (serpin B3/B4/B12/B13, calpastatin, SLPI, alpha-1 antitrypsin, serine protease inhibitor Kazal-type 7/5, and plasma serine protease inhibitor), inhibitors of cysteine proteases (capastatin and cystatin A/B), and inhibitors of other proteases (secretory leukocyte protease inhibitor (SLPI) and WAP four-disulfide core domain protein 2) were also major components of normative CVF [28]. Many of these proteins have immunological functions [28]. However, several of these inhibitors of neutrophil elastase activity, including leukocyte elastase inhibitor, alpha-1-antitrypsin and SLPI, along with others including alpha-1-antichymotrypsin were also identified in the vaginal fluid of women with signs of preterm labor [29]. Elastase inhibitors may act to protect the epithelial barriers from the effects of elastases released due to infection [30]. Many of the proteins identified in this study were plasma proteins, epithelial structural proteins and immunoregulatory proteins, some of which have been linked to intra-amniotic infection [29]. Proteins linked to host defense mechanisms were identified in vaginal fluid from women with signs of preterm labor including antimicrobial proteins (lysosome C, lactoferrin, NGAL, and von Ebner's minor salivary gland protein) and immunomodulatory proteins (annexin A1 and calgranulins A and B) were identified in vaginal fluid

from women with signs of preterm labor [29]. Lactoferrin, which was found in both normative [28] and preterm CVF [29], and transferrin, which was identified in preterm CVF [29], are iron-binding proteins that inhibit bacterial growth by reducing the available iron [31]. NGAL, which was also identified in the vaginal fluid of women with preterm labor, has been linked to infections related to preterm birth when found in AF [29]. Based on previous work, proteins with antimicrobial, defense, and immunological functions seem to be an important component of the CVF proteome.

Several studies have attempted to characterize the amniotic fluid proteome. Tsangaris et al. [32] identified 136 proteins in amniotic fluid at the time of genetic amniocentesis (16-18 weeks), many of which were regulatory proteins, enzymes, binding proteins, or had transportation functions. Their study also showed that amniotic fluid contains proteins of both maternal and fetal origin. Not surprisingly, albumin was the most abundant protein identified in this study, followed by alpha-1 antitrypsin, serotransferrin, immunoglobulin heavy chain, Ig kappa chain C region, fibronectin, and Vitamin D-binding protein. Immunoregulatory and extracellular matrix proteins were also identified, demonstrating the importance of the AF to the immune protection of the fetus and the maintenance of tissue integrity. Another study identified the amniotic fluid proteome as being dominated by enzymes, structural proteins, proteins with transport functions, signal transduction proteins, and chaperones [33]. Additionally, 6 members of the annexin family were observed [33]. In AF from term pregnancies, Park et al. [34], identified albumin, apolipoprotein, alpha-1-antitrypsin, serotransferrin, hemoglobin α/β chain, profilin I, actin, peptidyl-prolyl cis-trans isomerase A, and cytokeratin 1, among others. They also identified Calgranulin A and B in the AF of women with amniotic infection, but not in the AF of uninfected women. The amniotic fluid proteome likely reflects secretions from the fetal membranes (among other things including secretions from the baby and other tissues) and thus is an indicator of the state of the membranes. Alternately, changes

in the AF composition such as over- or under-expression of certain proteins or cytokines may affect the fetal membranes and lead to rupture.

Characterization of the fetal membranes, while not directly useful as a diagnostic tool, likely gives the most promise for directly identifying mechanisms important to PPROM. Hopkinson et al. [35] studied the proteome of amnion that had been prepared for human transplantation (often to help with burn or wound healing). The proteins that they found were mainly localized within the cytoskeleton, cellular organelles, or were extracellular proteins. This study found thrombospondin-1, which has functions in cellular adhesion, migration, apoptosis, wound repair, inflammation, and angiogenesis. Mimecan, a proteoglycan in the ECM which helps maintain tensile strength and hydration of tissues, was also identified in amnion. Integrin α6, which is involved in cell-matrix adhesion, was found in amnion tissue. Additionally, heat shock proteins and annexins, which have been implicated in wound healing and inflammation, were identified in amnion. Park et al. [34] identified several calcium-binding proteins within the soluble fraction of the amnion including calmodulin, annexins A1 and A2, macrophage-capping protein, and TGF-β-induced protein IG-H3, among others. Peroxiredoxins and galectins, both related to apoptosis, were also observed. Considering the structure of the amnion and that it is known to exhibit an inflammatory response (see section 1.5), the identification of many proteins related to tissue structural integrity, wound healing and inflammation in amnion is not surprising. The proteome of isolated chorion is not reported in the literature and thus requires further study. As previously described, the chorionic proteome and secretome may play an important role in membrane maintenance and degradation.

### 1.5. Inflammation and membrane rupture

Links have been made between inflammation and membrane rupture and labor. For example, inflammatory cytokines may lead to cervical ripening and the maturation of the chorioamnion [3],

leading to labor and membrane rupture. Much of the work in this area has been focused on the amniotic fluid, as it is likely that AF, rather than other maternal fluids, is more directly related to the inflammatory response in the fetus [3]. Women with intra-amniotic inflammation (as determined by SELDI-TOF identification of the inflammatory biomarkers defensins 1 and 2 and calgranulins A and C as well as histology), delivered at an earlier gestational age than those without intra-amniotic inflammation [1]. Interleukin-6 (IL-6) seems to be a reliable proteomic indicator of intra-amniotic inflammation and possible preterm birth [1]. Neonates born to women with severe intra-amniotic inflammation had higher cord blood IL-6 levels and more frequently had Early Onset Neonatal Sepsis (EONS) [1]. Moreover, the severity of neutrophilic infiltrate in the chorionic plate, choriodecidua, and the umbilical cord, but not the amnion, was able to predict the cord blood-to-AF IL-6 ratio [1]. The difficulty in predicting PPROM and preterm birth that may occur due to intra-amniotic inflammation is that even subclinical levels of inflammation may heighten risk and are difficult to detect. For example, 39% of neonates born to women with minimal intra-amniotic inflammation had above average IL-6 levels in their cord blood [1]. Infection is a frequent, although not the only, factor cited in intra-amniotic inflammation.

### 1.6. Infection and membrane rupture

Infections, both systemic and localized, have been implicated in membrane rupture. Inflammation (see section 1.5 'Inflammation and membrane rupture') caused by infections may play a role in some cases of PPROM. Evidence that supports infection as playing a role in labor includes: bacterial inoculation induces abortion or labor in animal studies, systemic maternal infections have been associated with the initiation of labor, and localized intrauterine infection has been associated with preterm labor [36]. Infections and their bacterial products such as lipopolysaccharide likely cause the release of inflammatory cytokines [3]. Onset of labor with bacterial infection has been

explained by the stimulation of prostaglandin biosynthesis by bacterial products [36]. Endotoxin (lipopolysaccharide) is present in the AF of women with intra-amniotic infection [37], and endotoxin can stimulate prostaglandin synthesis in the amnion and the decidua [38]. Amniotic fluid concentration of some prostaglandins (PGE2 and PGF2) are increased in women with intra-amniotic infection and PPROM with labor [36]. Bacterial endotoxin also causes the release of tumor necrosis factor (TNF) and interleukin-1 (IL-1) [36]. IL-1 induces collagenase activity, among other things. [36]. Macrophages are activated by microbial products such as IL-1, IL-6 and TNF [36]. TNF is also secreted by macrophages and is similar to IL-1 [36]. It stimulated prostaglandin production in amnion and decidua and is present in AF of women with intraamniotic infection and preterm labor, but is not present in normal AF [39]. IL-6, among other things, may induce the production of C-Reactive Protein (CRP), elevated levels of which in maternal serum precedes clinical chorioamnionitis and preterm labor for women with PPROM [40]. The peptides human beta defensins 2 (HBD2) and 3 (HBD3) are expressed in the amnion and the chorion [41]. Defensins are a family of antimicrobial cationic polypeptides that have antibacterial, antifungal, antiviral, and antiparasitic effects [42]. They are synthesized by epithelial cells and neutrophils, and they induce IL-8 synthesis [41]. HBD2 and HBD3 are expressed when cells are stimulated by proinflammatory cytokines including IL-1β, TNF-α and IFN-γ, and by microorganisms [41]. Iavazzo et al. showed that second semester amniotic fluid concentration of HBD2 positively correlated with PPROM due to subclinical chorioamnionitis, but not with preterm labor [41]. No correlation was found between HBD3 correlations and either preterm labor or PPROM [41]. Gravett et al. showed using amniotic fluid samples from women and primates with subclinical chorioamnionitis that insulin-like growth factor-binding protein 1 (IGFBP-1 and calgranulin B may be able to be used as biomarkers of intra-amniotic infection [43]. Patients with microbial infection of the amniotic cavity also had higher MMP-9 concentration in the AF than

patients without microbial infection regardless of membrane status (see section 1.7, 'The role of proteases and their inhibitors in PPROM') [44].

As expected, the biochemical changes described above in the presence of infection are reflected in the mechanical properties of the membranes. McGregor et al. [45] showed that increased inocula of collagenase-producing bacteria showed reduction in membrane strength, elasticity, and work to rupture, although only the reduction in membrane strength was significant. Moreover, a reduction in collagen could be seen with both light and electron microscopy [45]. It seems likely that one way that bacterial infection causes membrane rupture is through the production of collagenase because non-collagenase producing bacteria did not cause a reduction in membrane strength [45]. Several microorganisms that have been previously associated with membrane rupture are collagenase-producing [45]. These include streptococcus agalactiae, bacteroides melaninogenicus, enterobacteracea, and various other aerobic and anaerobic bacteria [45]. Host neutrophils and macrophages associated with the inflammatory response caused by microorganisms release various lysosomal proteases, particularly neutrophil elastase [45]. Neutrophil elastase is known to hydrolyze the type II collagen which lends the amnion strength and elasticity [45].

## 1.7. The role of proteases and their inhibitors in PPROM

As previously introduced, the maintenance of membrane strength requires a balance between the synthesis and degradation of the ECM proteins [3]. Two major groups of proteins that are important in this maintenance are the matrix metalloproteinases (MMPs) and the tissue inhibitors of metalloproteinases (TIMPs). Cell culture experiments have shown that placental syncytiotrophoblasts and amnion epithelial cells exclusively produced MMP-9, while chorion trophoblasts produced both MMP-2 and MMP-9 [46]. Amnion mesenchymal cells produce only MMP-2 [46]. The activity of proteases (including MMPs) is controlled by the fact that they are

synthesized in a proenzyme form and also by protease inhibitors, such as the TIMPs [47]. Proteases are involved in bone remodeling, wound repair, and normal cellular maintenance [47]. Proteases can have a significant negative effect on fetal membrane strength and elasticity [47]. Draper et al. demonstrated using fluorescent studies that protease activity in membranes with PPROM was increased 10- to 40-fold over control membranes [47]. They also determined that the major protease activity in prematurely rupturing membranes was at 92 kilodaltons, which is likely to be MMP-9 [47]. More bands were also seen in zymogram gel electrophoresis for fetal membranes from women who delivered after PPROM than in control membranes [47]. Matrix metalloproteinases are enzymes which degrade ECM macromolecules, typically collagens [44]. They are proteases which use $Zn^{++}$-dependent catalytic mechanisms [48]. The various MMPs degrade different macromolecules. Interstitial collagenase (MMP-1) attacks type I collagen and the gelatinases (MMP-2 and MMP-9) act on denatured collagen, type IV collagen (a component of the basement membrane) and proteoglycans [49]. Type III collagen is more efficiently cleaved by MMP-1 than type I collagen [4]. Type V collagen is resistant to most collagenases, except the gelatinases MMP-2 and MMP-9 and a limited number of other enzymes [4]. Significant increase in the concentration of MMP-9 in the amniotic fluid is associated with the rupture of nonlabored membranes [44]. Patients with PPROM were shown to have higher AF MMP-9 concentrations than patients with preterm labor but without PPROM who eventually delivered at term [44]. MMP-9 likely plays a role in membrane rupture in term and preterm cases [44]. MMP activity in general, but particularly that of MMP-9 was higher in the AF of women with normal labor and premature membrane rupture [49]. Alternately, another study found increased MMP-9 in both term and preterm labored fetal membranes as compared to nonlabored, but no difference in MMP-2 expression between labored and nonlabored tissues [46]. However, McLaren, et al. found that both pro-MMP-9 and pro-MMP-2 activity was increased in the cervical zone of post-labor samples as compared to pre-labor samples, although no

regional differences were observed in either pro-MMP-9 or pro-MMP-2 in the post-labor samples [22]. However, in pre-labor samples, pro-MMP-2 still showed no regional differences, although pro-MMP-9 levels were higher in the cervical zone than I the 'midzone' (midway between the placental edge and the cervical zone) [22]. In post-labor membranes additional bands corresponding to the active forms of MMP-2 and MMP-9 were detected [22]. Levels of MMP-9 showed a 16-fold increase in the midzone of labored membranes as opposed to that of pre-labor membranes [22]. Placental tissue showed the same trend, with term labored placenta showing higher MMP-9 levels than term nonlabored placenta [46]. Although most studies have focused on measuring differing levels of MMPs, it may be the changing ratio of MMP to TIMP-1 which facilitates collagen degradation [49], rather than simply an increase in MMP levels. TIMP-1 concentrations were not reduced in normal labor, but were in prematurely rupturing membranes; this may represent a difference in the mechanisms between normal membrane rupture and PPROM [49]. Vadillo-Ortega et al. [49]also concluded that changes in the collagenases MMP-1 and MMP-8 or in the tissue inhibitors of metalloproteinases TIMP-3 and TIMP-4 may have a role in PPROM. Although changes in MMP-1 were not observed in the amniotic fluid, MMP-1 may be tightly bound to the chorioamnion ECM and thus may not be observed in the AF [49]. It is clear that a balance of the elements controlling ECM degradation, particularly MMPs and TIMPs, play an important role in membrane rupture. The trophoblast layer of the chorion produced MMP-9 [11], and thus study of the changing proteome of the chorion near the rupture initiation site is vital to a thorough understanding of rupture.

### 1.8. Biomarker discovery

Finding biomarkers indicative of future preterm labor and/or PPROM would be invaluable to the ability of clinicians to predict and prevent them. As previously described, indicators of infection or inflammation, as well as matrix metalloproteinases and their inhibitors have potential for use as

biomarkers. Additionally, serum markers of oxidative stress were increased in the CVF women in labor as opposed to those without labor [50]. Differentially expressed proteins were also associated with protease inhibition (cystatin-A), anti-inflammatory cytokine activity (interleukin-1 receptor antagonist), and oxidative stress defense (glutathione S-transferase, peroxiredixon-2, thioredoxin, copper-zinc superoxide dismutase, and epidermal fatty-acid binding protein) [50]. Cystatin-A, IL-1 receptor antagonist, epidermal fatty-acid binding protein, thioredoxin and copper-zinc superoxide dismutase displayed reduced expression in the labor group [50]. Glutathione S-transferase P and peroxiredoxin-2 were increased in labor [50]. The IL-1 receptor antagonist is an inhibitor of the proinflammatory cytokines IL-1α and β [50]. IL-1 receptor antagonist may counteract the proinflammatory effects of IL-1β during pregnancy [51]. Cystatin-A inhibits cysteine proteinases including cathepsins B, H, and L [50]. Cathepsin L is involved in ECM remodeling [50]. Kim et al. [52] established that bone morphogenetic protein 2 (BMP2) RNA and protein expression were increased significantly in patients at term with spontaneous labor versus those not in labor at term [52]. BMP2 messenger RNA and protein expression were also increased in patients with preterm labor with histologic chorioamnionitis versus those with preterm labor without histologic chorioamnionitis [52]. Butt, et al. used gel electrophoresis and mass spectrometry to find 56 proteins that appeared differentially expressed between preterm and term placentae, of which 11 were present in either only preterm or term samples [53]. All eleven of these proteins fit into three main functional groups: structural/cytoskeletal proteins, endoplasmic reticulum proteins with enzymatic/chaperone functions, and anticoagulant proteins and included keratin, various actins, vimentin, endoplasmin, and transgelin [53]. If biomarkers indicative of PPROM are discovered, it would greatly improve clinicians' ability to predict and prevent rupture. Ideally, these biomarkers would be present in CVF as it can be sampled less invasively and with less risk than other fluids and tissues. However,

identifying differentially expressed proteins where they are more abundant, such as in the placenta, fetal membranes or amniotic fluid, may facilitate their identification in the more dilute CVF.

## 1.9. Introduction to proteomics

The proteome is the "protein complement to the genome" [54]. It is relevant to study the proteome rather than the genome alone because the latter only accounts for a small percentage of all biological process [3]. The proteins are important functional biomolecules that execute many of the tasks required within the cell. As of yet, functional genomics has not answered many of the questions regarding PPROM and preterm parturition and identification of genes intrinsic to parturition is recognized as a difficult task [3]. Posttranslational modifications affect how a particular protein functions, and these modifications cannot (at least as of yet) be determined by the genome. Inhibition of the translation of some gene sequences and protein degradation of recently generated proteins mean that gene expression and protein expression levels often do not match. mRNA levels often also fail to match protein expression levels due to differing stabilities and translation efficiencies [54]. As opposed to other traditional methods of studying proteins such as gel electrophoresis and Western blot, a mass spectrometry-based proteomics approach allows researchers to study how proteins are changing on a global scale and in relation to one another, rather than just on an individual basis. This is important because some proteins serve regulatory, chaperone, and signal transduction functions and thus their expression levels may indirectly affect the levels of various other proteins and ultimately alter biological function. The typical flow of a mass spectrometry-based proteomics experiment can be seen in Figure 2. The protein population does not necessarily need to come from a cell culture, as shown in the image. In this study, the protein population was obtained from tissue lysates. Often, the proteins are separated prior to digest; however, this study uses a shotgun approach in which all of the proteins are digested into a

highly complex mixture. Various other preparation steps may be required, but basically the proteins must be digested using an enzyme, typically trypsin. The peptides are then separated using chromatography before entering the mass spectrometer. The ionization and mass analysis are described in detail below. Finally, various bioinformatics tools are used to determine the proteins present in the sample. Improvements in mass spectrometers as well as the development of peptide databases and bioinformatics tools have allowed mass spectrometry to become a powerful and effective tool in proteomics.

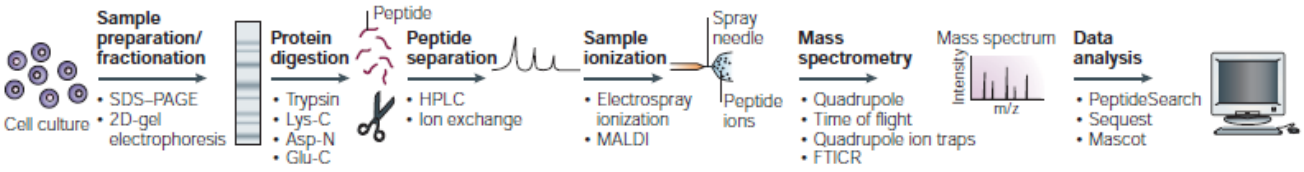


Figure 2: Flow of a mass spectrometry-based proteomics experiment [55].

## 1.10. Basics of mass spectrometry

Mass spectrometry is a method used to measure the mass-to-charge ratio of ions. It can be used to determine the composition and structure of sample materials. There are three major components involved in the process: ionization, mass analysis and ion detection. These three steps are described in-depth below. Prior to ionization, the sample can be fractionated using a variety of methods. Proteins can be separated using 2D gel electrophoresis and gel spots subsequently digested. Alternately, so-called 'shotgun proteomics' can be used to directly analyze complex solutions of proteins. In this method, complex protein digests are first separated, often using high performance liquid chromatography (HPLC). This approach is advantageous because it allows the identification of a large number of proteins within a complex sample rather than just a few. It also has advantages over other techniques such as Western blots in that, again, a large number of proteins can be identified, giving rise to an overall characterization of the proteome, and the investigators are able

to discover proteins that are present that they did not necessary anticipate being present. This is particularly applicable to the study of the chorion since very little study of the chorionic proteome has been completed up to this point.

### 1.10.1. Electrospray ionization

In order to analyze a material using mass spectrometry, it first must be ionized. Several methods of ionization are available including electron, chemical, thermospray, and matrix-assisted laser desorption/ionization (MALDI). However, electrospray ionization has become one of the most popular for use with biological samples and was used in this study. Electrospray ionization is often used to couple high performance liquid chromatography (HPLC) to a mass spectrometer and can be used when the material of interest is in a liquid matrix. [56]

The method of operation of electrospray ionization is show in Figure 3 below. A solvent typically containing a 1:1 mixture of water and an organic solvent such as methanol, acetonitrile or isopropanol plus <1% acetic or other acid, flows through a stainless steel capillary tube. Typical solvent flow rates range from 2-5 µL/min. The sample is injected into this stream and a large potential (3-4 kV) is applied between the capillary tip and the surrounding walls. This potential creates a field that causes the solution to break into a many fine, charged droplets. The solvent mixture is evaporated off the droplets with the help of a bath gas such as nitrogen. [56] The bath gas provides the thermal energy necessary for solvent evaporation [57]. For biological samples, nanoelectrospray (nanoES) is often used. In nanoES, the tip aperture is reduced to 1-3µm, flowrates are lowered to 20-40µL/min, and sample volumes can be as low as 1µL [56]. the low flowrate allows for signal accumulation and higher sensitivity [56]. Different materials, including fused silica, are also used for needles to avoid binding of biological samples to the needle surface.

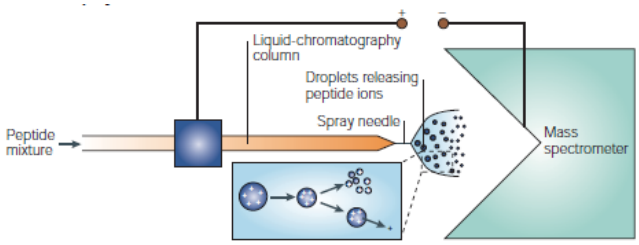


Figure 3: Electrospray ionization [55].

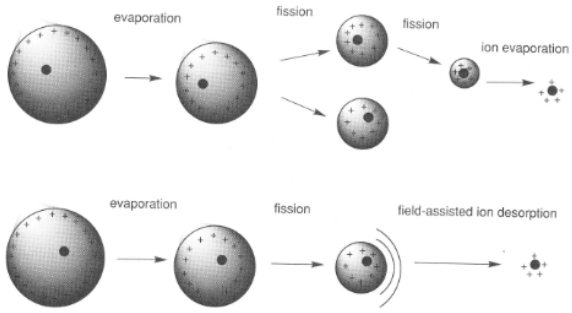


Figure 4: Ion evaporation model (IEM, top) versus charged residue model (CRM, bottom) [56].

There are two different widely accepted models for the mechanism of formation of gas-phase ions from the fine mist of charged droplets exiting the capillary tube. The first is called the Charged Residue Model (CRM). In the CRM model, the droplets continuously shrink in size as the solvent within them evaporates. This causes their surface charge density to increase to the Rayleigh instability limit, where Coulombic repulsion causes the droplet to break apart into smaller droplets. This sequence repeats until the droplets contain only one analyte molecule each. [56] This process can be shown in the bottom image of Figure 4 above.

The second model proposed for ion formation is the Ion Evaporation Model (IEM). In IEM, the same sequence of solvent evaporation and fission as described for CRM occurs. However, before the droplets become small enough to contain only one analyte molecule, much of the droplet charge escapes. This 'ion evaporation' is predicted to occur rather than Coulomb fission when the droplet radius is decreased beyond 10 nm. [57]The IEM process is shown in the top image of Figure 4 above.

### 1.10.2. Mass analysis

The mass analyzer is the central component of the mass spectrometry system as it achieves the critical goal of measuring the mass-to-charge ratio of the sample fragments. The

ionized fragments entering the mass analyzer are separated according to their mass-to-charge ratio. The mechanism for accomplishing this depends on the type of mass analyzer being used. Types of mass analyzers include magnetic sector, quadrupole, quadrupole ion trap, and time-of-flight, among others. The analyzer used in this study was a quadrupole ion trap and as such quadrupoles alone will be described in detail. Four performance parameters are used to evaluate mass analyzers[58]. The first is the range of masses that the analyzer can handle. The second is the resolution, or the ability to distinguish ions with adjacent masses. The third parameter is the scan speed. A quick scan speed is needed to observe the material eluting off the HPLC column as well as other fast changing events, while a slow scan speed provides better mass measurements. Finally, the detection sensitivity, or the smallest amount of sample that can be detected, is an important parameter.

The quadrupole is one of the most popular mass analyzers currently used. Electric fields are used to manipulate and separate ions. The quadrupole consists of four parallel rods arranged in a square configuration. A direct current (dc) potential (U) and a radio frequency (rf) potential ($V\cos\omega t$) is applied to one pair of the rods (where V is the amplitude of the rf signal, t is time and ω is the angular frequency of the signal). The other pair of rods receives a dc signal of –U and an rf signal of $-(U-V\cos\omega t)$, which is 180° out of phase with the rf signal on the first pair. The combination of these applied potentials creates an oscillating field within the quadrupole. As ions are injected along the axes of the rods, only those ions within a specific range of mass-to-charge ratios will have stable trajectories allowing them to move through the analyzer. In this matter, the quadrupole acts as a band-pass filter. The field is varied to allow different ranges of ions to pass through the analyzer. [58]

Quadrupole ion-trap mass spectrometers operate using some of the same principles as the quadrupoles described above. However, they control ions in time, not in space. The ion-trap contains three electrodes: a doughnut-shaped electrode in the center and two end-cap electrodes. A combination of dc and rf voltages that allows a wide m/z range to be within the trap is applied. The magnitudes U and V and the frequency ω is then continuously increased, causing the trajectories of ions with higher and higher m/z ratios to become unstable. They then exit the trap through an opening in one of the end-cap electrodes and move toward the detector. [58]

### 1.10.3. Detection

After being separated in the mass analyzer, the mass and abundance of the ions [58] (the ion current), must be detected. Focal point detectors detect ions one at a time, while focal plane detectors detect all of the ions arriving along a plane at the same time [58]. The instrument in this study used a continuous channel electron multiplier (CEM) detector. These detectors take advantage of the fact that when a fast-moving ion strikes certain surfaces, electrons are emitted [58]. The emitted electrons then accelerate and strike the next surface they reach, causing the emission or more electrons and so on [58]. This creates gain for the signal. In a CEM, these collisions are occurring within a horn-shaped glass tube doped with lead or coated with beryllium, into which the ion beam is introduced [58].

### 1.10.4. Tandem mass spectrometry

Tandem mass spectrometry (MS/MS or $MS^2$) is a method used to obtain structural information about the sample by coupling two mass spectrometers either in space or in time. The three steps in MS/MS are: mass selection, fragmentation, and mass analysis. Various types of scans are possible in MS/MS experiments including the product and precursor ion scans.

Product ion scans are the most common. In such a scan, the MS/MS spectrum is the result of the fragmentation of specific, mass-selected precursor ions.[59]

The precursor ion can be fragmented in a number of different ways, with collision-induced dissociation (CID) being used most often. In CID, energy from the field excites the precursor ion. This causes collisions of the ion with a collision gas to become more intense and more frequent, causing the ion to fragment. [60] The ion fragments are then detected, producing the MS/MS spectrum.

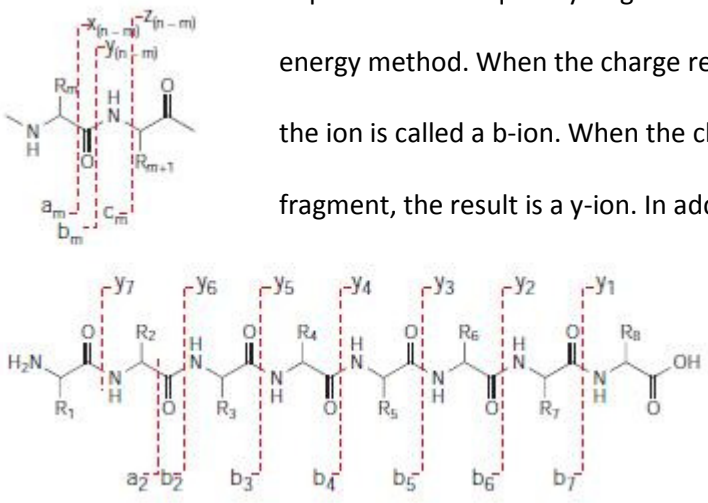


Figure 5: Peptide structure and fragment designation [55].

Peptides most frequently fragment at the amide bonds as this is the lowest energy method. When the charge remains on the amino-terminal fragment, the ion is called a b-ion. When the charge remains on the carboxy-terminal fragment, the result is a y-ion. In addition to b- and y-ions, a-ions can occur when a C=O group is lost from a b-ion and additional alterations can occur due to the loss of a $NH_3$ or $H_2O$ group. The a-, b-, and c-ions are numbered from the original amino terminus, while x-, y- and z-ions are labeled from the original carboxyl terminus. This scheme can be seen in Figure 5. [55]

### 1.10.5. Protein Identification

Generally, the goal of proteomics experiments ultimately involves the identification of the proteins present in the sample, either for overall sample characterization or for use in drawing conclusions about the changing proteome under altered experimental conditions. Protein identification is most often accomplished using tandem mass spectrometry (MS/MS) data and

database searching. As described in detail in section 1.10.4, the tandem mass spectrometry spectrum consists of the m/z ratios and intensities for all of the fragment ions produced by the fragmentation of a particular precursor ion. Several commercial database search tools have been developed to automate the process of identifying the peptides responsible for a tandem mass spectrum and ultimately the protein from which they came. These include SEQUEST, Mascot, and X!Tandem, among others. Mascot and X!Tandem were used in this study. Although the algorithms used by these programs are generally proprietary, they all work in a similar manner. They compare the tandem mass spectrum to a database of theoretical fragmentation patterns of peptides and find matches between them [61]. Multiple possible matches can be identified and are scored according to their probability of being the correct match.

Databases have been developed by various institutions for many different species. Commonly used databases include the National Center for Biotechnology Information (NCBI) Entrez Protein database, Uniprot (consisting of the combined Swiss-Prot and TrEMBL databases), the International Protein Index (IPI) database and the NCBI Reference Sequence database (RefSeq), among others. The different databases vary in the species available, the degree of redundancy present within the database and their annotation. [61]

As previously described, the tandem mass spectrum consists of peaks due to a series of ions, with each ion differing from its neighbor by one amino acid. This allows the identification of the amino acid sequence by determining the mass difference between adjacent peaks in the series and comparing it to the known weights of the various amino acids. However, in reality the mass spectrum often is missing some peaks and also may have intervening peaks which may not be part of the series [55]. Protein identification by database searching helps alleviate this problem because it is not necessary to be able to clearly identify each amino acid directly from

the MS/MS spectrum. Rather, the ion fragments that are actually observed are compared to the expected fragments based on protein fragmentation chemistry [55]. The Mascot search engine uses probability-based matching. It determines the theoretically-predicted peptide fragments for all the peptides within the database being searched and matches them with the experimentally-observed fragments (Figure 6) [55]. The 'identification score' for each matched peptide fragment is the negative logarithm of the probability that the number of fragment matches is random multiplied by 10 [55].

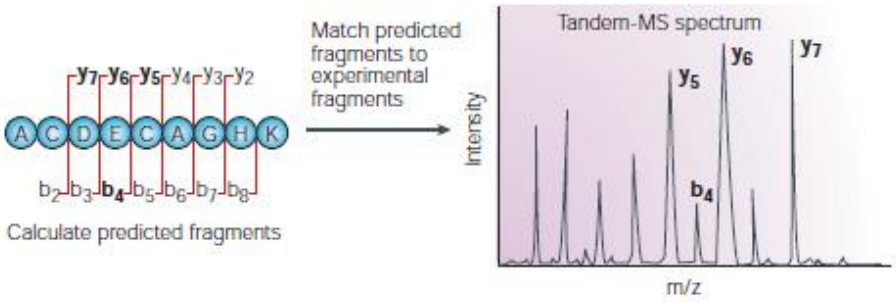


Figure 6: Database matching in Mascot [55].

### 1.10.6. False identification rate

In order to statistically validate the peptide identifications obtained through database searching, the false identification is often used. A common method of determining the false identification rate is through reversed database searching. The reversed entries will have no real matches and thus can give an estimation of the false positive rate. It is then assumed that the same number of random matches occur in the forward (normal) database [61]. The total number of incorrect matches is then $2N_{rev}$. In all cases the peptide assignments (matches) are only counted if they have a score above a specific chosen threshold. The total number of peptide assignments is: $N_{tot} = N_{rev} + N_{norm}$ [61]. The false identification rate can then be calculated as: $Err = (2*N_{rev})/N_{tot}$ [61].

### 1.10.7. Label-free, relative quantitation

Researchers often want to not only identify the proteins present in a sample, but also to determine their quantities, or at least their relative quantities for different experimental conditions. While the intensity of the signal of a peptide ion does not directly reflect the amount of protein present in the sample due to differing accessibility to the protease, peptide solubility and ionization efficiency, the peak height can be used to determine the relative amount of a given protein between experiments [55]. Often, relative quantitation is carried out using stable isotope tags. However, label-free, relative quantitation can also be accomplished. Although it is generally considered less accurate than quantitation using stable isotopes [62], it does have some significant advantages. Labeling methods necessitate expensive isotope labels, expertise in interpreting the data, specific software, and they limit the number of samples that can be quantitated in a given experiment [62]. In many proteomics experiments, and particularly in biomarker discovery, it is important to look at how many proteins are changing together, on a global level, rather than individually [62], as in traditional quantitation methods. The two basic label-free methods are: (1) area under the curve (AUC) and (2) spectral counting (SC) [62]. In AUC, the area under the peak of the chromatogram for the precursor ion is integrated and is linearly proportional to the concentration of the peptide [62]. SC uses the idea that more abundant peptides are fragmented more frequently for MS/MS and thus will have a higher abundance of MS/MS spectra than lower abundance peptides [62]. More abundant proteins will produce peptides that are detected more often and also provide more full protein coverage than those from less abundant proteins. This means that in data-dependent MS/MS, the spectral count will be proportional to the protein concentration [62]. Often a normalization factor is employed to improve the accuracy. The SC method with normalization is used in this study and is described in '*Materials and methods*'. In order to test the ability of label-free

shotgun proteomics to detect differentially expressed proteins, Zhang et al. [63] spiked bacterial lysates with known concentrations of protein markers. They then employed several statistical tests and evaluated their ability to identify the differentially expressed proteins and the associated false positive rate. For the G-test, Fisher's exact test, and AC test, which do not require replicates, the spectral count data for the replicates were pooled. The statistical tests that do require replicates were the t-test and LPE test. The only differentially expressed proteins were the spiked markers. Large differences (10- and 5-fold) in the spiked protein levels were successfully detected by all tests with low false positive rates. A 2-fold change resulted in a greater than 10% false positive rate for tests requiring only one replicate. For less than three replicates, Fisher's, AC, and G-test all gave fairly good results. Despite a sacrifice in accuracy, label-free quantitation methods can overcome some of the disadvantages associated with labeled methods and can be an effective method of identifying differential protein expression.

2. Motivation & objectives

As previously described, preterm birth is a major cause of perinatal morbidity and mortality and also contributes to continuing health problems. Preterm premature rupture of the membranes (PPROM) is a significant cause of preterm birth. As presented in the *Introduction*, although certain conditions including infection, inflammation, and protease-induced ECM degradation are understood to contribute to rupture, the overall mechanisms underlying PPROM remain unknown. Additionally, most of the research that has been completed up to this point has been on the amnion layer; thus little is known about the characteristics of the isolated chorion. While this makes sense based on the relative strengths of the layers, the chorion may actually be quite important to the maintenance of chorioamnion. There is evidence that an element of the chorion's secretome acts to weaken the amnion [19]. The delamination of the chorioamnion also reduces membrane strength [8]. An overall understanding of membrane

rupture and its subsequent application in clinical diagnoses and treatments is not possible without a thorough understanding of the chorionic layer. This research aims to characterize the proteome of the chorionic layer of the fetal membranes. Additionally, relative quantitation of protein expression levels between the regions proximal to and distal from the rupture initiation site will identify differentially expressed proteins and possible biomarkers for PPROM. Collagen and glycosaminoglycan (GAG) content in both regions will be evaluated using biochemical assays and will also be visualized using stained histology images.

## 3. Materials and methods

### 3.1. Sample collection

Fetal membranes were obtained from deliveries at the University of Colorado Hospital in Aurora, CO. Women were informed of this research study and agreed to participate at will. They signed an informed consent before the membranes were collected. This study did not affect normal care. This research was conducted under the approved protocol COMIRB #06-1159.

Fetal membranes were collected from women with both spontaneous rupture (SROM) and artificial rupture (AROM) of the membranes at term (37+ weeks gestational age) delivering vaginally. None of the membranes in the study were obtained from patients with a known pregnancy-related condition (i.e. preeclampsia, gestational diabetes, etc.). Biopsies were excised both proximal to and distal from the rupture initiation site as identified by the delivering physician. The chorion and amnion layers were separated, flash frozen in liquid nitrogen and stored at -80°C for future preparation. Anita Kramer, Dr. Virginia Winn, Brandi Briggs, Meghan Donnelly, Dr. Karen Jonscher and I carried out the sample collection and labeling.

### 3.2. Lysate preparation

In order to prepare the samples, a known mass of sample was pulverized in liquid nitrogen with a mortar and pestle. Tools were also kept cool in liquid nitrogen. The pulverized sample was mixed with chaotropic lysis buffer (7M urea, 2M thiourea, 4% CHAPs) with 100 µl 100mM dithiothreitol (DTT), 10 µl protease inhibitors (GE), and 2 µl ampholytes added to each milliliter of buffer. The chaotropic lysis buffer disrupts the cell membrane and macromolecular structures. For samples weighing between 50 and 100 mg, 500 µl of buffer was added. The samples were homogenized with a sonicator and then incubated on ice for 45 minutes. Samples were then centrifuged for 30 minutes at 14000 *rcf* and 4°C. Lysates were then aliquoted into 50 and 100 µl aliquots and stored at -80°C until further use.

### 3.3. Quantitation

Lysate protein concentration was determined using the Bradford method, a colorimetric assay. Standards were created using bovine serum albumin (BSA) in chaotropic lysis buffer. Standards and samples were all diluted 1:1 with HPLC-grade water to reduce the urea and thiourea concentrations below the threshold for the Bradford reagent. Samples were then diluted with a water/buffer mixture (1:1 mixture of chaotropic lysis buffer and HPLC-grade water) to keep the buffer concentrations consistent to create 4- and 8-fold dilutions. 5 µl of standard or sample plus 250 µl of room temperature Bradford reagent was added to the appropriate well. The wells were mixed and bubbles within the wells were removed. The optical density was read on a spectrophotometer. A standards curve was created in Excel and used to calculate the concentration of the samples. If both dilutions fell within the range of the standards, the concentrations from the two dilutions were averaged. Otherwise, the dilution that fell within the range of the standards was considered accurate (standards range was chosen based on the Bio-Rad Bradford Assay datasheet).

After detergent removal and protein precipitation (see Section 3.4), a second quantitation was performed using the BCA method. Standards were created using BSA in 8M urea in 100mM ammonium bicarbonate buffer. Standards and samples were diluted to reduce the urea concentration to below 3M (the threshold for the BCA working reagent, 7 parts standard or samples: 13 parts HPLC-grade water). Samples were then diluted with a water/buffer mixture (7:13 mixture of buffer and HPLC-grade water). 10 µl of standard or sample plus 200 µl of BCA working reagent was added to the appropriate well. The plate was incubated at 37°C with gentle agitation for 30 minutes, and the optical density was read on a spectrophotometer. A standards curve was created in Excel and used to calculate the concentration of the samples. As described for the Bradford quantitation, the dilutions which best fell into the range of the standards was use.

3.4. Detergent removal and protein precipitation

Prior to mass spectrometry, the lysates were run through detergent removal columns (Pierce) to remove the CHAPs detergent from the lysis buffer. The detergent produces a strong signal and elutes at the same time as more hydrophobic peptides. Thus, many of the hydrophobic peptides (those with lower signals than the CHAPs) would not be detected. In order to avoid this, the detergent must be removed.

The protein content was precipitated using a 2D clean-up kit (GE Healthcare). This separates the proteins and allows the removal of any residual detergent, salts, nucleic acids, and lipids. The precipitated protein pellet was rehydrated with 8M urea in 100mM ammonium bicarbonate.

A volume of lysate containing 120 µg of protein as determined by the Bradford quantitation (see above) was used to determine the volume of lysate for detergent removal and protein precipitation. Approximately 50% loss of total protein was assumed throughout both clean-up steps. The protein pellet was rehydrated in 60 µl of 8M urea in 100mM ammonium bicarbonate to yield a protein

concentration of approximately 1 µg/µl. When the volume for 120 µg of total protein fell outside of the allowable volume for the spin columns, the closest allowable volume was used and the rehydration volume was adjusted accordingly.

### 3.5. Digest

An in-solution digest process was carried out on the rehydrated samples. Samples (30µL) were alkylated and reduced using 200mM iodoacetamide and 1M DTT respectively. These steps function to linearize the protein and prevent it from refolding. The samples were then digested using 1mg/mL trypsin overnight. Digestion was stopped using 1 µL of 100% formic acid. Trypsin cleaves the protein at specific points in the amino acid sequence yielding a complex mixture of peptide fragments. BCA protein quantitation was carried out on a portion of the rehydrated samples (prior to digestion) to accurately determine the protein concentration after detergent removal and 2D cleanup.

### 3.6. Mass spectrometry

Based on the BCA protein quantitation, the volume of sample digest required to yield 1.0 µg total protein was calculated and loaded for mass spectrometry analysis. Samples were run by Joe Gomez at the Mass Spectrometry core facility at the Skaggs School of Pharmacy and Pharmaceutical Sciences at the Anschutz Medical Campus. The instrument is a 3D quadrupole ion trap. This instrument's nano-pump separates the complex peptide mixture first by basicity (strong cation exchange) and then by size (reversed phase). Nine salt fractions were yielded for each sample and the nine output files were later combined. Prior to running the samples, Mr. Gomez dehydrated the samples and rehydrated them with 0.1% formic acid because he was concerned that the ammonium bicarbonate would interfere with the strong cation exchange separation.

3.7. Bioinformatics workflow

The bioinformatics and data analysis workflow is the part of the methodology that allows identification of the proteins present in the sample, grouping of these proteins into functional and cellular compartmental groups, and identification of any proteins exhibiting differential expression. The instrument output was converted to a Mascot Generic File (MGF) for each salt fraction. The files were then searched against databases of protein sequence data using Mascot (Matrix Science). Mascot uses the mass from the peptide fragmentation spectra to identify all the proteins within a given database that could yield the peptide. Further constraints, such as requiring the peptide to be tryptic (as was the case in this study) and choosing as tight of a mass tolerance as is reasonable for the instrument used, are then applied. The fragment ion masses are compared to the expected masses to choose the best match, which is then mapped back to the protein from which is likely came. The search database was the human database obtained from the UniProt Knowledgebase concatenated with a database of common contaminants that was downloaded from the Matrix Science website. The database was then reversed and concatenated with itself within Scaffold (Proteome Software; 227,622 entries). The reversed entries will have no real matches and thus can give an estimation of the false positive rate. The Mascot search was carried out with precursor tolerance of 1.2u, fragment ion tolerance of 0.6u, selecting trypsin as the digestion enzyme and allowing up to 2 missed cleavages, and the appropriate modifications (carbamidomethylation and methionine oxidation). The Mascot searches yielded DAT files for further evaluation.

Scaffold 3.0(Proteome Software) was used to further analyze the files and to facilitate comparison between samples. A minimum of 2 peptides with a probability of 50% and a protein probability of 80% were required to make a protein identification. Within Scaffold, the unweighted spectral count (the number of times a particular protein was identified from the mass spectrometry

data) was used to calculate the quantitative value. The quantitative value is a normalized spectral count which can be used to adjust for run-to-run variance. The calculation of the normalized spectral count is demonstrated in the following example. Assume you have two biosamples: A and B. Both of the two biosamples contains three proteins: Protein 1, Protein 2 and Protein 3. Protein 1 has 12 spectra in Biosample A and 8 spectra in Biosample B. Protein 2 has 6 spectra in Biosample A and 3 spectra in Biosample B. Protein 3 has 4 spectra in Biosample A and 3 spectra in Biosample B. Biosample A has 22 spectra total. Biosample B has 14 spectra total. The average number of spectra per sample is 18. These values are used to construct a normalization factor which can be multiplied by the unweighted spectral count to yield the quantitative value. The normalization factor is the average spectral count divided by the number of spectral counts for the biosample. For all of the proteins in Biosample A, the unweighted spectral count is multiplied by 18/22. For all of the proteins in Biosample B, the unweighted spectral count is multiplied by 18/14. [64]

In order to look for differential protein expression, the Mann-Whitney U test was used on the normalized spectral counts (the quantitative values as described above). P-values up to 0.100 (90% confidence) were identified as potentially differentially expressed because due to the small sample size, only a few proteins met the criteria for 95% confidence. With larger sample sizes, it is likely that these proteins would reach statistical significance with a p-value below 0.050, and thus increasing the type I error slightly was an acceptable trade-off for not excluding potentially interesting proteins. Other statistical tests for significance (such as the Student's t-test) were considered for determining differential expression. However, in general they require larger sample sizes or normally distributed samples. Although at least one study has shown the t-test to yield reasonable results in detecting differential protein expression [63], these tests are not really valid for use in this study.

The Functional Annotation tool within the Database for Annotation, Visualization and Integrated Discovery (DAVID; http://david.abcc.ncifcrf.gov) was used to classify the biological processes and cellular compartments to which the identified proteins belong. First, the UniProt accession numbers corresponding to the identified proteins were converted to a list of Unigene gene identifiers using UniProt's ID Mapping tool (www.uniprot.org). A small number of proteins could not be mapped. The Unigene list was loaded into the DAVID Functional Annotation tool. The default selections were deselected and the Biological Processes and Cellular Compartment Gene Ontology categories were selected in subsequent analyses. The clusters from the DAVID output were used to create categories showing the percentage of the identified proteins involved in certain types of biological processes and located within certain cellular compartments. [65], [66]

### 3.8. Biochemical assays

In order to further characterize biochemical changes in the membranes, collagen and proteoglycan quantities were determined using biochemical assays. Collagen was quantified by a biochemical assay directly measuring hydroxyproline. The quantity of collagen present in the sample can be determined by multiplying the hydroxyproline quantity by 7.2. Biopsy punches were excised from both the placental and rupture regions using an 8.0mm diameter biopsy punch. Duplicate samples were run for each region. The tissues were lyophilized for 6 hours. Prior to lyophilization, both the samples and the lyophilizer flask were frozen in the -85°C freezer for at least 20 minutes. Once the samples were dried, the dry weights were recorded and the samples were added to a tube with 5mL of 6M HCl. The samples were hydrolyzed in an oven at 108°C for 18 hours. The hydrolyzate was then decanted and the tubes washed thoroughly with deionized water. 60mL of deionized water (including the water used for washing) was combined with the hydrolyzate, yielding 75mL. Several drops of 0.02% methyl red indicator and 12mL of 2.5M NaOH were added to each sample.

The pH was then adjusted to between 6 and 7 using 1M HCl and 2.5M NaOH. The volumes of acid and base added during the neutralization process were carefully tracked. Neutralized samples were stored at 4°C for up to one month. [67]

Hydroxyproline standards with concentrations of 0, 1.5, and 2.5 µg/mL were prepared in 2mL volumes. The previously neutralized samples and standards were aliquoted out into 2mL quantities in test tubes. Hydroxyproline oxidation was initiated by adding a 1mL quantity of chloramine-T solution (0.05M chloramine-T in 20mL deionized water, 30mL Methyl Cellusolve, and 50mL buffer (50g citric acid monohydrate, 12mL glacial acetic acid, 120g sodium acetate trihydrate, and 34g sodium hydroxide brought up to 1L in deionized water with the pH adjusted to 6.0)) and the tubes were incubated at room temperature for 20 minutes. Chloramine-T was then destroyed with 1mL 3.15M perchloric acid and the tubes were incubated at room temperature for 5 minutes. P-dimethylaminobenzaldehyde (20% solution in Methyl Cellusolve) was added in a quantity of 1mL and the tubes were incubated in a water bath at 60°C for 20 minutes. Tubes were then cooled in cool tap water for 5 minutes and pipetted into a 96-well plate (200µL of sample per well). All additions were made in the same order and contents were thoroughly mixed by vortex after each addition. The absorbencies were read on a spectrophotometer at 557nm. Collagen content was calculated and expressed as percent dry weight.[67]

Sulfated glycosaminoglycan content was quantified using a dimethyl methylene blue (DMMB) assay. As previously described, samples were excised from each region using an 8.0mm biopsy punch and were lyophilized. Dry weights were recorded and the sample was added to an Eppendorf tube with 500µL digestion buffer (100mM sodium phosphate/10mM $Na_2EDTA$/10mM L-cysteine/0.125mg/mL papain enzyme, filter sterilized using a 0.22µm filter). Tubes were vortexed and incubated at 60°C for 18-24 hours. Chondroitin sulfate standards were prepared in buffer

(100mM sodium phosphate/10mM $Na_2EDTA$). Following digestion, samples were again vortexed. In a 96-well plate, 10µL of standard or samples was mixed with 250µL of DMMB solution (16.0mg DMMB/3.04g glycine/2.37g NaCl/5.2mL 100% ethanol/deionized water to 1L and pH adjusted to 3.00).The absorbencies were read at 515nm.

3.9. Histology

Collagen and cellular content was visualized using Masson's Trichrome staining. In Masson's Trichrome, collagen stains blue, while the cytoplasm stains red. Masson's Trichrome-stained images were used to identify the layers of the chorioamnion (amnion, chorion (reticular layer), trophoblast layer and decidua), to compare the collagen content between regions, and to take thickness measurements. For thickness measurements, the area of chorion cross section was taken as well as the length of the length of the two edges ($d_o$ and $d_i$ in Figure 8). The area was divided by the average of the lengths to yield the average thickness of the section. Measurements were taken in ImageJ. Only the thickness of the reticular layer (labeled 'C' in Figure 7 below) was taken into account, although the trophoblast layer is often considered part of the chorion. The reasons for this were two-fold. First, pathologists do not include the trophoblast layer when examining tissues for chorioamnionitis. Second, the amount of attached trophoblast and decidual layers varied greatly and is affected by maternal, environmental and tissue processing factors. Thus, large differences that are completely unrelated to the region or mode of rupture would be seen if the trophoblast layer was included. Areas that appeared to have fractured within the chorion layer were avoided if possible to avoid artificially large thickness measurements. Slides were stained in a Leica autostainer.

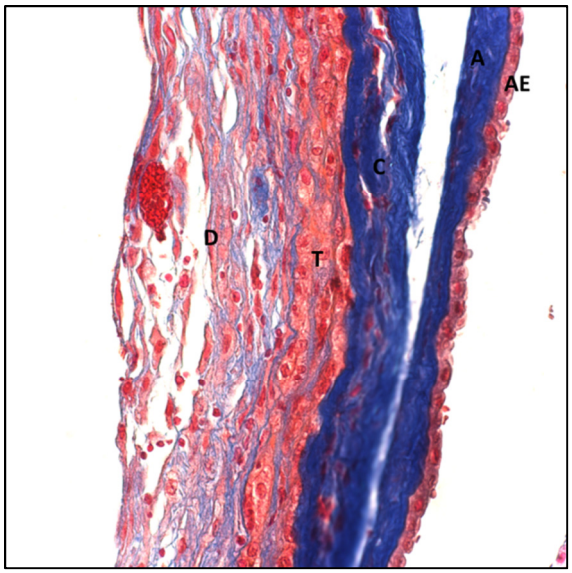


Figure 7: Layers of the chorioamnion in a Masson's Trichrome stained image. AE: amniotic epithelium, A: amnion, C: chorion (reticular layer), T: trophoblast, D: decidua

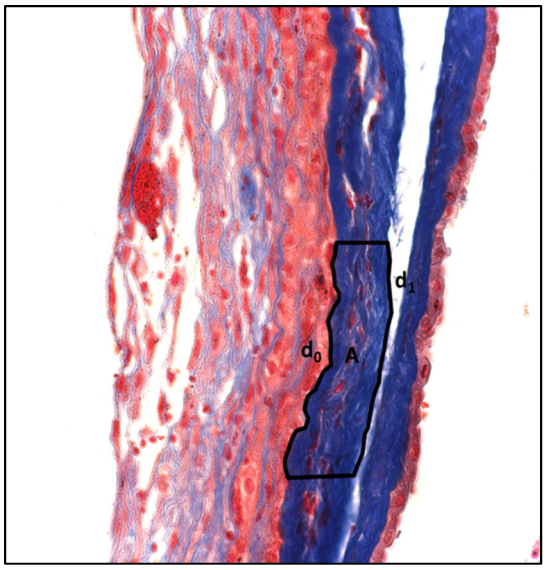


Figure 8: Method for taking thickness measurements in ImageJ.

Proteoglycans were visualized using Safranin O/Fast Green staining. This protocol stains proteoglycan content red and the background green. Safranin O-stained images were used to compare proteoglycan content between samples. Images were stained by hand according to the protocol in Appendix X.

## 4. Results

### 4.1. Proteomics

Using the acceptance criteria described in 'Methods,' 227 proteins were identified in the chorion samples. The 50 most abundant proteins are listed in Figure 9 below. The false discovery rate was 0.4%. As previously described, DAVID was used to categorize the proteins identified in the chorion samples. The distribution of these proteins by biological function is shown in Figure 10 below.

| | Protein | Accession | Molecular Weight |
|---|---|---|---|
| 1 | Albumin | A8K9P0 | 69 kDa |
| 2 | Beta globin (Fragment) | Q4TWB7 | 11 kDa |
| 3 | Beta-globin | C8C504 | 16 kDa |
| 4 | Uncharacterized protein | E9PE77 | 256 kDa |
| 5 | Vimentin | P08670 | 54 kDa |
| 6 | Actin, cytoplasmic 1 | P60709 | 42 kDa |
| 7 | Fibrinogen beta chain | P02675 | 56 kDa |
| 8 | Keratin, type I cytoskeletal 19 | P08727 | 44 kDa |
| 9 | Keratin, type II cytoskeletal 8 | P05787 | 54 kDa |
| 10 | Hemoglobin alpha-1 globin chain (Fragment) | E9M4D4 | 11 kDa |
| 11 | Annexin A2 | P07355 | 39 kDa |
| 12 | Protein-glutamine gamma-glutamyltransferase 2 | P21980 | 77 kDa |
| 13 | Fibrinogen gamma chain | P02679 | 52 kDa |
| 14 | Alpha-1-antitrypsin | P01009 | 47 kDa |
| 15 | Lumican | P51884 | 38 kDa |
| 16 | Collagen alpha-3(VI) chain | P12111 | 344 kDa |
| 17 | Fibrillin 1 | D2JYH6 | 312 kDa |
| 18 | G-gamma globin Paulinia variant | D3GKD9 | 16 kDa |
| 19 | Alpha-1 thalassemia globin gene (Fragment) | P78461 | 9 kDa |
| 20 | Glyceraldehyde-3-phosphate dehydrogenase | P04406 | 36 kDa |
| 21 | Putative uncharacterized protein | Q6N089 | 52 kDa |
| 22 | IGK@ protein | Q6PIL8 | 26 kDa |
| 23 | Apolipoprotein A-I | P02647 | 31 kDa |
| 24 | Transferrin variant (Fragment) | Q53H26 | 77 kDa |
| 25 | Alpha-enolase | P06733 | 47 kDa |
| 26 | Keratin, type I cytoskeletal 18 | P05783 | 48 kDa |
| 27 | Protein S100-A11 | P31949 | 12 kDa |
| 28 | Fibrinogen, A alpha polypeptide (FGA), transcriptvariant alpha, mRNA | A8K3E4 | 70 kDa |
| 29 | Keratin, type II cytoskeletal 7 | P08729 | 51 kDa |
| 30 | Annexin A1 | P04083 | 39 kDa |
| 31 | Keratin 6A (KRT6A), mRNA | A8K2I0 | 60 kDa |
| 32 | Vitronectin | P04004 | 54 kDa |
| 33 | Galectin-1 | P09382 | 15 kDa |
| 34 | Keratin, type I cytoskeletal 14 | P02533 | 52 kDa |
| 35 | cDNA FLJ78587 | A8JZY9 | 50 kDa |
| 36 | Peptidyl-prolyl cis-trans isomerase | A8K486 | 18 kDa |
| 37 | Tubulin beta-7 chain | B7ZAF0 | 47 kDa |
| 38 | Actin, alpha, cardiac muscle (ACTC), mRNA | A8K3K1 | 42 kDa |
| 39 | Triosephosphate isomerase | D3DUS9 | 31 kDa |
| 40 | Transgelin-2 | P37802 | 22 kDa |
| 41 | Macrophage migration inhibitory factor | P14174 | 12 kDa |
| 42 | Protein disulfide-isomerase | P07237 | 57 kDa |
| 43 | Pyruvate kinase isozymes M1/M2 | P14618 | 58 kDa |
| 44 | Transforming growth factor-beta-induced protein ig-h3 | Q15582 | 75 kDa |
| 45 | Complement C3 | P01024 | 187 kDa |
| 46 | Collagen alpha-2(VI) chain | P12110 | 109 kDa |
| 47 | Endoplasmin | P14625 | 92 kDa |
| 48 | Collagen alpha-1(VI) chain | P12109 | 109 kDa |
| 49 | IGL@ protein | Q8N355 | 25 kDa |
| 50 | Phosphoglycerate kinase 1 | P00558 | 45 kDa |

Figure 9: 50 most abundant proteins identified in the chorion samples.

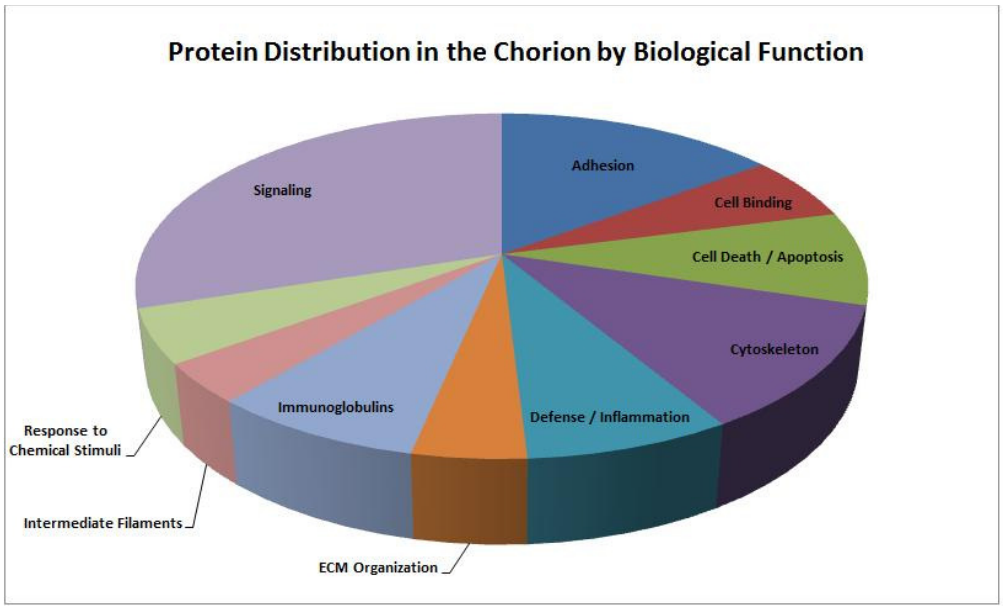


Figure 10: Distribution of chorion proteins by related biological process.

Protein expression was compared between the artificially rupturing and spontaneously rupturing membranes as previously described using the Mann-Whitney U test. None of the identified proteins were shown to exhibit statistically different expression ($p<0.05$) across the different mode of rupture groups. Only approximately 7% of the identified proteins had $p<0.100$ and in all cases they had a p-values of 0.095. Thus, the artificially rupturing groups (AROM) and spontaneously rupturing membranes (SROM) were assumed to come from the same population and were combined for subsequent analyses.

Using the Mann-Whitney U test and allowing p-values up to 0.100, 14 proteins were identified as potentially differentially expressed between the placental and rupture regions. Three of these met the more stringent 95% significance level. The potentially differentially expressed proteins and their Uniprot accession numbers are listed in Table 1 below along with a brief description of their function in biological processes from the Uniprot Knowledgebase [68]. The protein content of the membranes was also evaluated based purely on the presence or lack of presence in the group. If a

protein was found in 80% of the samples for a particular group, it was considered present in that group (although for the SROM group, a 50% cutoff had to be used since n=2). More proteins were present exclusively in the rupture region than the placental region and these proteins were more often upregulated in rupture. Additionally, more proteins were observed exclusively in AROM membranes than in SROM membranes. Several basement membrane-specific proteins including fibrillin and laminin were seen exclusively in AROM membranes across both regions. The proteoglycans decorin, laminin, and nidogen were observed exclusively in AROM rupture, but not SROM rupture. Fibrinogen was seen in AROM but not in SROM membranes. Finally, talin and vinculin, proteins involved in focal adhesions, were observed only in AROM rupture.

| ***Accession*** | ***Protein Name*** | ***Description*** | ***Up/Down in Rupture*** |
|---|---|---|---|
| Q5I6Y6 | Lamin | Intermediate filaments | Up |
| P02042 | Hemoglobin subunit | Oxygen binding and transport | Up |
| A8K3E4 | Fibrinogen | Platelet activation, protein polymerization, signal transduction | Down |
| P02675 | Fibrinogen beta chain | Platelet activation, protein polymerization, signal transduction | Down |
| P78461 | Alpha-1 thalassemia | Oxygen binding and transport | Up |
| P02647 | Apolipoprotein A-I | Cholesterol/lipid/steroid transport and metabolism | Up |
| P31949 | Protein S100-A11 | Negative regulation of cell proliferation, signal transduction | Up |
| B7ZAF0 | Tubulin | Microtubules | Up |
| P14174 | Macrophage migration inhibitory factor | Proinflammatory cytokine, regulation of macrophage activation | Up |
| P10909 | Clusterin | Apoptosis, immune response | Down |
| Q0QEN7 | ATP synthase subunit | ATP synthesis | Up |
| B3KY95 | Protein disulfide isomerase A6 | Homeostasis, metabolic processes | Up |
| B4DE02 | Annexin A4 | Calcium ion binding, inflammation, apoptosis, membrane scaffolding | Up |
| P27105 | Erythrocyte band 7 integral protein | Cation transport, integral membrane protein, cytoskeleton | Up |

Table 1: Differentially expressed proteins. Highlighted entries met 95% significance level. Others met 90% significance.

The differentially expressed proteins were clustered in DAVID. The differentially expressed proteins clustered into three categories: Assembly, Wound Response, and Immune Response. Wound response was the largest cluster.

4.2. Biochemical Assays

Collagen content was measured by quantitating hydroxyproline content as described above. No significant regional differences were seen in collagen content between tissues taken from proximal to and distal from the rupture initiation site. In addition, no pair-wise trends (when comparing the placental and rupture tissues for a particular sample) were observed. The coefficients of variance achieved between replicates were generally quite small, but a fairly large variation in collagen content was seen across samples from the same region. One sample was excluded because it exhibited issues with repeatability indicative of problems during sample processing. Another sample was excluded because it exhibited extremely high collagen levels, indicating that it perhaps had been contaminated (possibly the amnion layer was not fully separated during sample collection). The regional collagen concentrations (expressed as micrograms of collagen per milligrams of dry weight) are shown in Figure 11.

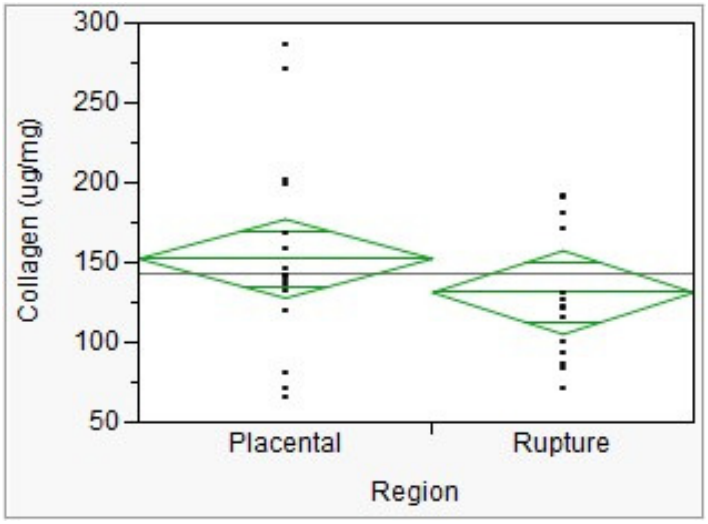


Figure 11: Collagen content by region with 95% confidence intervals.

Proteoglycan content was measured by quantitating sulfated glycosaminoglycan (sGAG) content with the DMMB assay as described above. No significant regional differences in sGAG content were observed between tissue from the rupture and placental regions. However, in observing the pair-wise relationships (between the placental and rupture region tissues for a particular sample), 6 out of 7 samples showed a reduction in sGAG content in the rupture region tissue, although the change was generally small. The sample that showed an increase in sGAG content in the rupture region had a rupture region sGAG concentration that was ~47% above the overall rupture region average, while the placental region value for the same sample was only ~7% above the overall placental region average. The regional sGAG concentrations (expressed as percent of dry weight) are shown in Figures 12 and 13. Additionally, amongst the placental region tissues, sGAG was significantly reduced in the SROM membranes versus the AROM membranes. This reduction did not hold for the rupture region tissues (Figure 14).

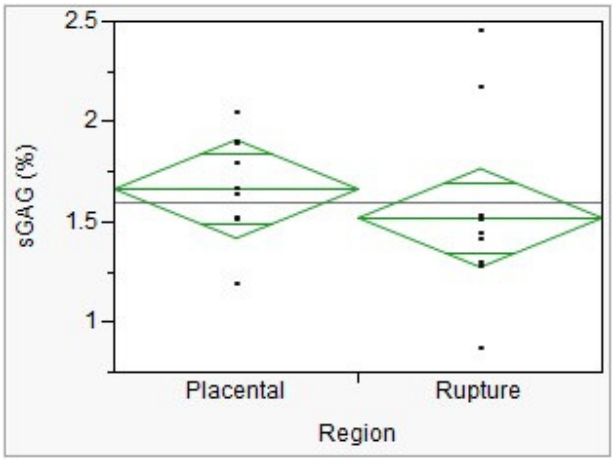


Figure 12: sGAG content of SROM membranes with 95% confidence intervals.

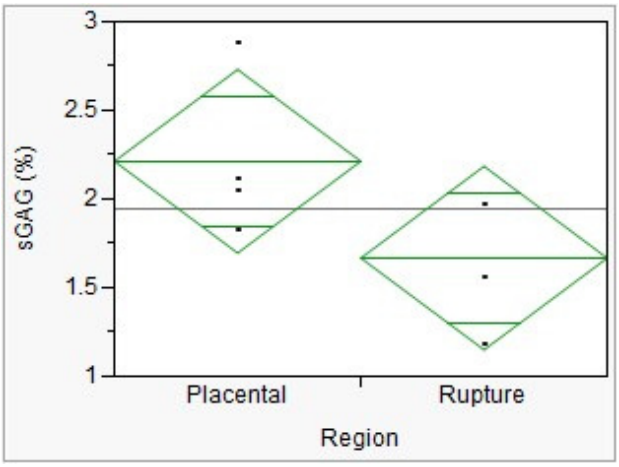


Figure 13: sGAG content by region of AROM membranes with 95% confidence intervals.

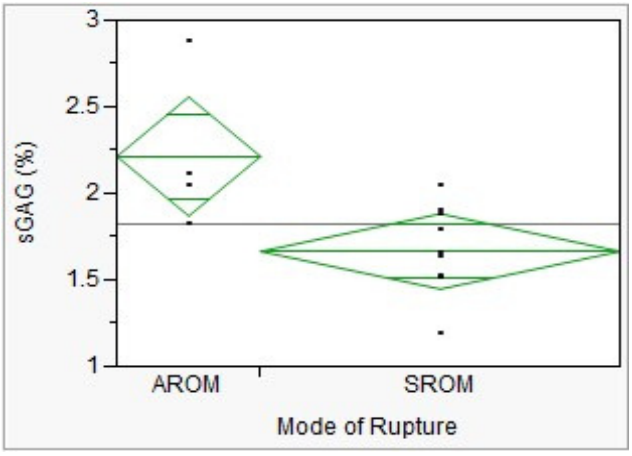


Figure 14: sGAG content of placental region tissue by rupture mode.

## 4.3. Histology

Masson's Trichrome stained slides were used to obtain images for thickness measurements of the chorion layer as described above. An increase in thickness of the chorion in the rupture region was observed, although the difference did not reach significance. The overall standard deviation was high, reaching almost one third of the mean value for each region. This is not surprising considering the variability of human tissues and the error reported on thickness measurements in the literature. The overall average thickness for the placental region was 40.2 μm ± 9.8 μm, while the overall average thickness for the rupture region was 47.6 μm ± 19.9 μm (reporting error as 95% confidence intervals). In a pair-wise comparison (between the placental and rupture region tissues for a particular sample), 3 out of 4 of the samples also showed an increased chorion thickness in the rupture region. Interestingly, the one sample that did not exhibit this increase was the one in which chorioamnion damage made it difficult to measure and 2 out of the 3 placental slides could not be measured because the 'shredding' seen in the chorioamnion made distinguishing between the layers impossible. Slides were then categorized by their ease of measurement and thus the likelihood that a good measurement was obtained. The categories were as follows: 1: 'easy to measure', 2: 'somewhat difficult to measure', 3: 'impossible to measure'. The main reason for a slide to receive a rating other than 1 was damage to the chorioamnion. According to Dr. Miriam Post, a pathologist specializing in obstetric and gynecologic pathology, damage to the amnion is quite common and is probably more likely to be caused by delivery and tissue sample processing than to be indicative of any actual changes to the tissues. Therefore, excluding the difficult to measure slides will likely improve the quality of the measurements as opposed to excluding samples indicative of a change within the tissues. When only slides categorized as '1s' were taken into account, the means for the placental and rupture regions exhibited further separation, but the

difference was still not significant. The thickness for the placental region was 35.8 μm ± 8.8 μm, while that for the rupture region was 47.9 μm ± 19.9 μm.

Masson's Trichrome stained slides were studied for qualitative differences in the staining intensity or distribution. No clear regional differences were observed in the Masson's Trichrome stained slides. The intensity of blue staining for collagen appeared approximately equivalent between regions, particularly in the reticular chorion layer. There was some evidence of reduced blue staining for collagen within the decidua in the rupture region. However, since the presence and appearance of the decidua varies greatly between slides due mostly to conditions related to the delivery and processing of the tissue for histology, no conclusions can be drawn from this evidence. Red stained cellular content was observed interspersed within the blue collagen of the reticular layer of the chorion and did not differ by region. As described above, the layers were fairly easy to distinguish in the Masson's Trichrome stained images. In many cases, the amniotic epithelium layer was missing, although as previously discussed, this likely was not indicative of any real change within the tissues. It did not appear to be more likely to occur in one region than the other. When present, the amniotic epithelium appeared as a distinct, red-stained layer of columnar cells on the inner-facing (away from the chorion) edge of the collagenous amnion. The cells dispersed throughout the amnion and the reticular layer of the chorion, mostly fibroblasts, were more irregular in shape, but in general were elongated parallel to the layer boundaries. The cells within the trophoblast and decidual layers were large and fairly round. Although hematoxylin is used in the Masson's Trichrome staining sequence and thus the nuclei are stained, the intensity of red and blue staining makes it difficult to evaluate nuclei morphology. The appearance of the nuclei is important in looking for the multi-lobular nuclei of immune cells that are indicative of prechorioamnionitis and histologic chorioamnionitis. While none of the samples were obtained from patients diagnosed with clinical chorioamnionitis, there is poor correlation between clinical and histologic diagnoses of the condition

and thus histologic evidence may be seen in these samples. Hematoxylin and eosin (H&E) staining may be required to evaluate the presence of histologic chorioamnionitis. Representative images of Masson's Trichrome stained slides from the placental and rupture regions can be seen in Figures 15 and 16 below.

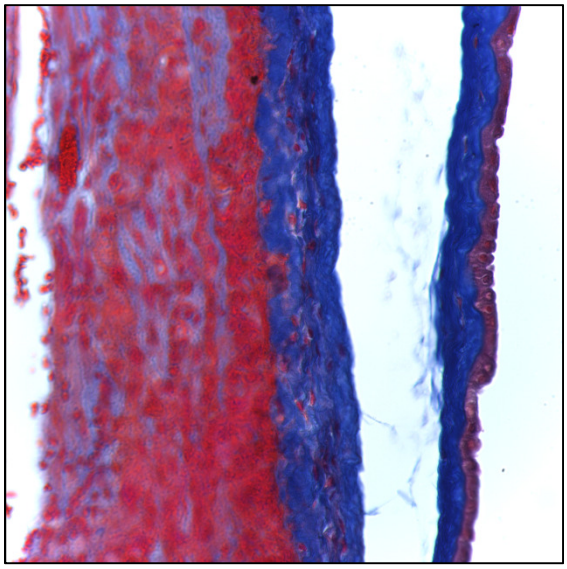

Figure 15: Masson's Trichrome stained image of the placental region (40x magnification).

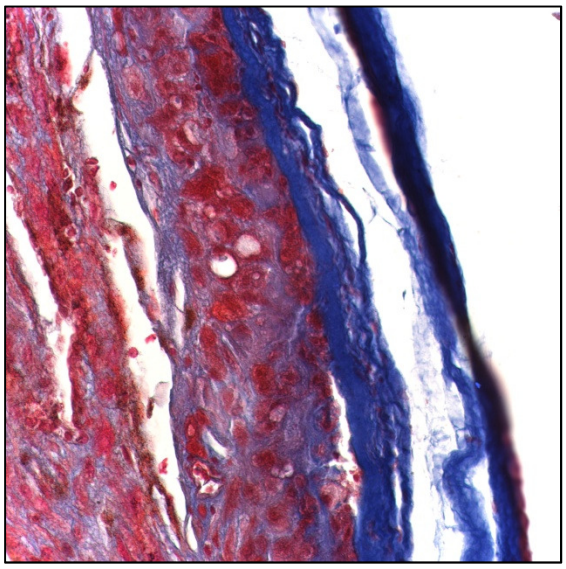

Figure 16: Masson's Trichrome stained image of the rupture region (40x magnification).

An interesting feature in many of the Masson's Trichrome stained images was the presence of ghost villi. These appeared as oval, blue-stained regions within the trophoblast layer (Figure 17). According to Dr. Post, the ghost villi are placental villi that formed away from the placental disc and became entrapped within the membranes. Evidence of shear failure as shown by tears in the tissue parallel to the layer boundaries can also be seen in many of the samples.

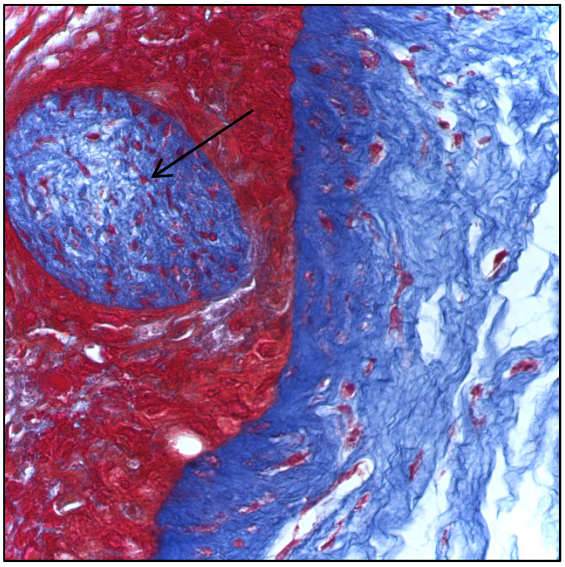

Figure 17: Ghost villi within the trophoblast layer (indicated with an arrow).

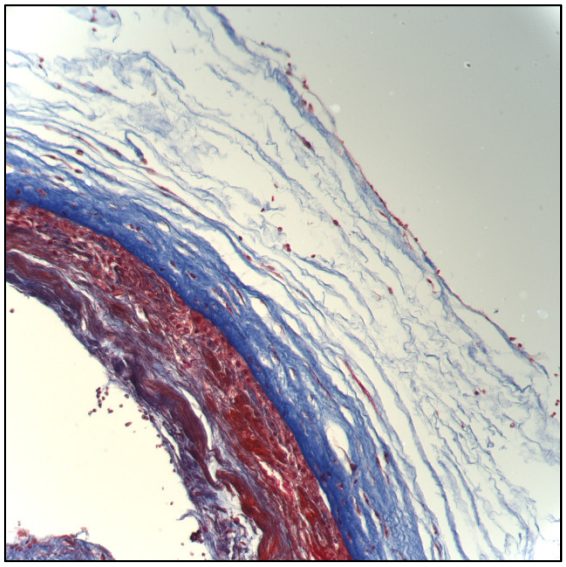

Figure 18: Damaged ('shredded') layers of the chorioamnion as seen in several slides.

Safranin O/Fast Green stained images were studied for qualitative differences in proteoglycan content. The layers are not as easily identifiable in these images as they were in the Masson's Trichrome stained images. Proteoglycan content stained red and the background content stained green. The intensity of the staining appeared equivalent across the placental and rupture regions. However, there appeared to generally be less green staining within the layers in the rupture region images than in the placental region images. This may be indicative of the presence of either less non-proteoglycan containing content in the rupture region or conversely of an increase in proteoglycan content which may be competing with and blocking the appearance of the Fast Green stain. As with the Masson's Trichrome stained images, fractures in the tissues could be seen, although in these images fractures both parallel and more perpendicular to the layer boundaries were observed. Additionally, the intensity of staining from slide to slide seemed to vary more than with the Masson's Trichrome. Within the tissue layers, the green content often appeared somewhat

greyish, while when it appeared more at the edges it was brighter green. This may have been due to competition with red staining of proteoglycan content with in the layers.

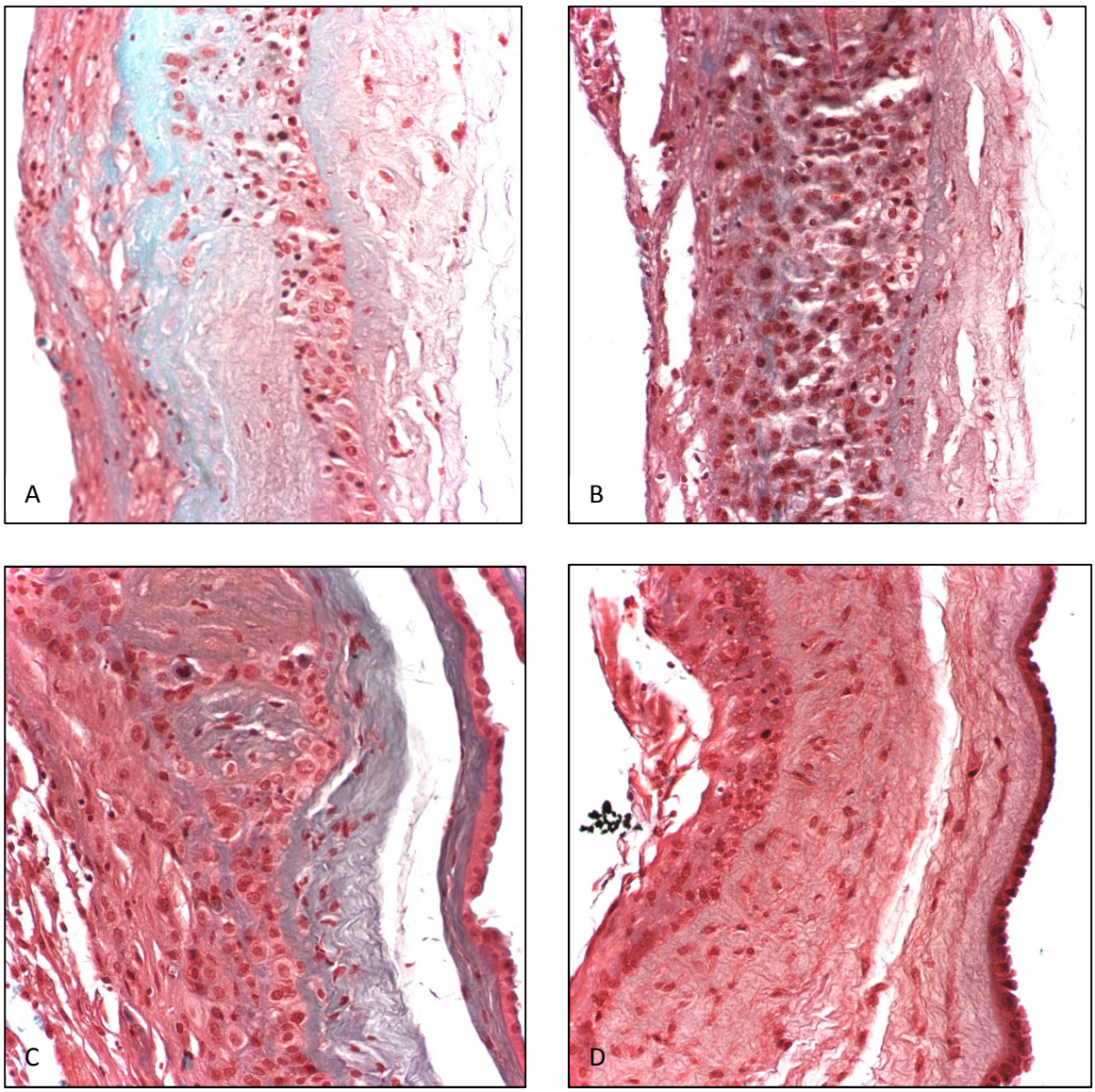


Figure 19: Safranin O/Fast Green stained images. A and C are from the placental region; B and D are from the rupture region. A and B are from one membrane, as are B and D.

# 5. Discussion

## 5.1. Proteomics

A large percentage of the chorion proteins were involved in signaling. This is not surprising considering that the cellular trophoblast layer was included in this analysis and considering evidence that the chorion appears to be indirectly causing amnion weakening [19]. Another large group of proteins was involved with cell and tissue structural integrity, including those involved specifically in adhesion, extracellular matrix organization, cell binding, and intermediate filaments. Another sizeable portion of chorion proteins are involved in defense and inflammation. As previously discussed, inflammation likely plays an important role in membrane rupture. Finally, smaller percentages of proteins are involved in cell death/apoptosis and response to chemical stimuli.

As expected, several types of collagen (collagen alpha-3 (VI), collagen alpha-2 (VI), collagen alpha-1 (VI), collagen alpha-1 (XIV), collagen type I alpha 1, collagen alpha-1 (IV), collagen alpha-2 (I), collagen alpha-1 (VII), collagen alpha-1 (I)) were identified in the chorion. From the literature and the hydroxyproline assays, we know that collagen is a major component of the chorion (~13-15% of the tissue dry weight). Thus, this result was expected. Unexpectedly, none of the matrix metalloproteinases and only one of the tissue inhibitors of matrix metalloproteinases (TIMP 3) were observed in the chorion. This was somewhat surprising due to their likely role in membrane rupture (see 1.7 ‘The role of proteases and their inhibitors in PPROM’). However, histology and hydroxyproline assay results indicate that collagen content is not changing within the chorion layer and thus the MMP and TIMP interactions may not play an important role in the chorion. Additionally, these proteins may be present but in lower abundances that were not able to be identified. Targeted proteomics looking specifically for MMPs and TIMPs or other targeted methods (Western blots, etc.) may be required to identify these proteins and changes in their abundances.

The proteins that were differentially expressed between the placental and rupture region tissues clustered into three groups: Assembly, Immune Response, and Wound Response. The abundance of the proteins within the functional groups did not necessarily change in the same way, however. The differentially expressed proteins clustered into groups related to biological processes that are important in the maintenance of tissue integrity.

Macrophage migration inhibitory factor was found to be upregulated in tissue from the rupture region. Macrophage migration inhibitory factor is a cytokine associated with inflammation and sepsis. It also has a function in wound repair [69],[70]. The concentration of macrophage migration inhibitory factor in amniotic fluid has been shown to increase with increasing gestational age and also in patients with chorioamnionitis [71]. However, the same study found no correlation between increased amniotic fluid concentrations of macrophage migration inhibitory factor and spontaneous term parturition. The increase in macrophage migration inhibitory factor in the rupture region in this study fits with this previous study in the context of inflammation and rupture, although it does not appear to be a direct cause of membrane rupture.

Protein S100-A11 (also called calgizzarin), which was upregulated in tissue from the rupture region, has been implicated in wound repair and regeneration [72]. Calgizzarin may be upregulated in the rupture region due to an attempt to repair damage to the tissues within the rupture region.

Fibrinogen and fibrinogen beta chain were both downregulated in tissue from the rupture region. Fibrinogen simulates normal clotting and is used in some commercially available tissue sealants and surgical glues [73],[74]. A reduction in fibrinogen in the tissue may then reduce the tissue integrity and promote membrane rupture.

Apolipoprotein A-I was upregulated in the rupture region tissue. It plays a role in limiting the damage caused by inflammation [75]. It may be present in larger concentrations in the rupture region tissue in an attempt to combat the increased inflammation present in the region.

Clusterin may help protect tissues by removing radicals and stopping oxidation [75]. It was downregulated in the rupture region tissue. This reduction in clusterin may encourage membrane rupture at the rupture site by allowing oxidative damage.

### 5.2. Biochemical Assays

The collagen content of the chorion found in this study for both the placental and rupture regions (147.1 μg/mg dry weight and 134.3 μg/mg dry weight respectively, or 14.7 and 13.4 percent of the dry weight) fit within the literature values of 12-15% [13]. Based on previous studies on MMP expression and activity in amnion (see section 1.7 'The role of proteases and their inhibitors in PPROM'), it was expected that collagen concentration would be decreased in the rupture region. Based on the results of this study, it may be that a decrease in the collagen content is seen in the amnion, but not in the chorion. This is logical since the amnion is the major load bearing component of the fetal membranes. Additionally, the protocol used in this study measured total collagen. Also of importance is the soluble, or extractable, collagen. Extractable collagen is the collagen content with a lesser degree of crosslinking [76]. Crosslinking density is associated with mechanical strength [77], so changes in extractable collagen rather than simply total collagen content may be responsible for the reduction of strength in the rupture region of the fetal membranes. Additionally, when investigating cervical collagen concentrations, Myers et al. observed a change in cervical collagen content between pregnant and non-pregnant tissues when comparing the collagen mass per tissue wet weight, but did not see a change when comparing the collagen mass per tissue dry weight [76]. This was due to the change in hydration levels seen between the pregnant and non-

pregnant tissues. There may be differing hydration levels and thus differing collagen content when comparing the collagen content per wet tissue weight over the placental and rupture regions. However, while wet weights were taken for all samples, the wet weight is greatly affected by the sample collection process. Although the membranes were continuously kept moist with phosphate buffered saline (PBS) throughout collection, the wet weight varied significantly depending on the amount of time that the membrane had been thawed and the amount of time since it was last sprayed with PBS. This effect was exaggerated due to the dry environment. Therefore, scaling by wet weight is unlikely to yield any useful conclusions.

The average sGAG content for all samples ranges from 1-3% of dry weight. It was difficult to compare to literature values because most previous studies reported quantities of specific proteoglycans and/or glycosaminoglycans as opposed to the total sulfated glycosaminoglycan content measured here and also report GAG content per wet tissue weight, which introduces the problems discussed above [14]. The only source reporting values of total sulfated glycosaminoglycans that was found was a masters thesis from 2006 [78]. This thesis reported a values of 188 ± 31 μg/mg dry tissue weight for average sulfated glycosaminoglycan in the chorion. This translates to 18.8% of dry weight, significantly higher than our results. However, this seems quite high. The GAG content of arteries has been reported as ~1.5-3% of tissue dry weight [79]. This result has been replicated in our lab using the same DMMB technique used in this study. Therefore, we have reasonable confidence in our technique and our results seem valid. No significant change in sGAG content was seen between the placental and rupture region tissues. Meinert et al. found an increase in biglycan and hyaluronan concentration and a decrease in decorin concentration in cervical amnion after delivery [8]. Hyaluronan is non-sulfated and thus will not be detected by the DMMB assay. Biglycan and decorin are both sulfated, but an increase in biglycan may be offset by a decrease in decorin, resulting in no total change in the sGAG content. Alternately, the sGAG

concentration may be changing in the amnion and not the chorion. Decorin enhances collagen organization while biglycan and decorin both upset it [8]. Thus, if future work shows that the soluble collagen content is remaining constant across regions in the chorion, this would provide evidence that concentrations of specific proteoglycans are not changing in the chorion. However, if soluble collagen levels are shown to increase in the rupture region tissue, this would support the idea that the chorion biglycan content is increasing while the decorin content decreases in such a way that the total sGAG content of the rupture tissue remains constant.

### 5.3. Histology

The Masson's Trichrome stained images yielded thickness measurements of 286 μm and 383 μm for the placental and rupture regions respectively. Oxlund et al. obtained measurements of 185 μm and 192 μm for fresh and stored chorion specimens respectively [80]. However, these measurements were obtained by sandwiching the membrane between pieces of glass and using a micrometer. The physical forces involved in this method may results in smaller thickness measurements. Halaburt et al. used a similar method and obtained values ranging from 318 μm near the placenta to 140 μm at the rupture site [13]. Both sets of measurements were completed on normal, term membranes, demonstrating the difficulty in taking such measurements and their inherent variability. Additionally, although it is not explicitly stated, due to the methods used, it is likely that these studies are including any attached trophoblast and decidual layers, while here we measured only the reticular layer of the chorion. It is interesting that Halaburt et al. reports a reduced thickness near the rupture site [13]. While it may seem intuitive that degradation at the rupture site would lead to reduced thickness, it has been documented in the literature that the supracervical weak zone is characterized by swelling and increased thickness [4], [22]. The trend in our data, while not reaching significance, agrees well with this. This swelling occurs in the

connective tissue specifically, while the trophoblast and decidual layers do thin [22], which may account for the decrease in thickness at the rupture site observed by Halaburt et al.

No qualitative change in collagen or cellular content was observed between the placental and rupture regions using the Masson's Trichrome stained images. This is consistent with the results of the hydroxyproline assay. Histology slides were only available for 4 SROM membranes, which precluded mode of rupture comparisons.

Although far from conclusive, it did appear that there was more proteoglycan content (as seen as a decrease in green-stained background content) in the rupture region than in the placental region using the Safranin O/Fast Green stained slides. This result was not supported by the results of the DMMB assay. However, the DMMB assay specifically measured sulfated glycosaminoglycans, whereas the Safranin O stains all proteoglycan content. Therefore, an increase of total proteoglycan content may be present in the rupture region whereas the sGAG content remains constant. As discussed, an increase in biglycan and hyaluronan and a decrease in decorin has been seen with delivery [8]. The extra hyaluronan is present in a gelatinous substance that forms between the layers of the chorioamnion and encourages delamination [8]. This increase in hyaluronan may be responsible for the possible appearance of increased proteoglycan content in the rupture region, although it appears to occur not only at the interface of the chorioamnion, but throughout the layers of the membranes.

## 6. Conclusions

Biochemical changes in the fetal membranes are likely related to changes in their mechanical properties leading to rupture. This study used mass spectrometry-based proteomics, biochemical assays, and histology to investigate differences in membranes based on mode of rupture (artificially vs. spontaneously rupturing) and region (placental region vs. rupture region). No differences in

protein expression were identified from membranes with different modes of rupture. Several proteins were potentially differentially expressed between the placental and rupture region tissues, although many of them did not reach a 95% significance level. The differentially expressed proteins were all involved in assembly, wound response, and immune response. The sample to sample variation in the proteomics data was quite high even within one experimental group. High variability is expected in biological tissue, but some of the regional changes associated with membrane rupture may be too subtle to reliably be seen above the noise. Additionally, many of the proteins thought to be associated with membrane rupture (MMPs, TIMPs) were not observed in this study. Although important, these proteins may be present in abundances too low to be captured with this method. Targeted mass spectrometry or other proteomics techniques may be required to capture changes in these proteins. No difference in collagen content was seen between the placental and rupture region tissues as evaluated by hydroxyproline assay. No difference in sulfated glycosaminoglycan content was observed between the placental and rupture region tissues as evaluated by DMMB assay. The sGAG content was reduced in SROM tissues as compared to AROM tissues, although the reduction was only significant within the placental group. Masson's Trichrome stained histology images corroborated the results of the hydroxyproline assay. A consistent increase in chorion thickness was observed in the rupture region tissue, although this increase did not reach significance. Safranin O/Fast Green stained histology images appeared to show a small increase in proteoglycan content in the rupture region. Hyaluronan (a non-sulfated glycosaminoglycan) may account for the discrepancy between the DMMB assay results and the histology images. Additionally, if an increase in proteoglycan content occurs at the interface between the amnion and the chorion, the additional proteoglycan content may attach to the amnion during separation. This study indicates that if a reduction in total collagen content leads to membrane rupture, it likely occurs in the amnion, an increase in proteoglycan content may be associated with rupture, and that

certain proteins associated with assembly, wound response and immune response are potentially differentially expressed in rupture tissue.

7. Future work

Further work is required to more fully understand the mechanisms underlying membrane rupture. Current work being performed in our lab will provide mechanical strength data, proteomics data, collagen content, and proteoglycan content on the amnion, giving a fuller picture of changes in the overall chorioamnion.

A larger sample size may help in achieving significance for differentially expressed proteins and thickness changes. Additionally, targeted proteomics or other more specific methods would allow the investigation of lower abundance proteins such as MMPs and TIMPs that likely play an important role in membrane rupture. Network analysis should also be performed to understand how groups of related proteins are changing together and to ascertain their possible roles in biological processes related to membrane rupture.

Quantitating the soluble collagen content within the chorioamnion would provide a better picture of changes to the load bearing collagen of the membranes that may lead to membrane rupture.

A more thorough and systematic approach to the thickness measurements as well as additional input from a pathologist would increase the confidence in the measurements. As described, multiple measurements were taken, but a more systematic approach in taking the images for measurements may improve the results. Additionally, I was not fully blinded to which sample an image came from, which would improve objectivity. Finally, histology images were only available for the spontaneously

rupturing membranes making it impossible to perform histologic comparisons based on mode of rupture, although based on other results, no changes are expected.

Co-expression network analysis, as suggested by Dr. Matt McQueen, may allow give a better understanding of how groups of proteins are changing together as well as the biological pathways in which they are involved. This type of analysis will give a better understanding of changes in the proteome than the more simplistic relative quantitation presented here. Network analysis is important because while individual proteins may not exhibit a large change in quantity, if groups of proteins are consistently changing in the same way, these changes may still be important to the mechanisms behind membrane rupture.

Finally, if possible, strength testing should be completed on the chorion. It would be helpful to look at the strength data alongside the proteomics data. Hopefully it will be possible to observe changes in particular proteins or networks of proteins that correlate with changes in mechanical strength.

# 8. Bibliography


[1] C. S. Buhimschi et al., “Fetal inflammatory response in women with proteomic biomarkers characteristic of intra-amniotic inflammation and preterm birth.,” *BJOG : An International Journal of Obstetrics and Gynaecology*, vol. 116, no. 2, pp. 257-67, Jan. 2009.

[2] B. M. Mercer, “Preterm premature rupture of the membranes: current approaches to evaluation and management.,” *Obstetrics and Gynecology*, vol. 101, no. 1, pp. 178-193, Sep. 2003.

[3] C. S. Buhimschi, C. P. Weiner, and I. A. Buhimschi, “Proteomics , Part II : The Emerging Role Spontaneous Preterm Labor / Birth,” *Obstetrical and Gynecological Survey*, vol. 61, no. 8, pp. 543-553, 2006.

[4] J. F. Strauss, “Extracellular Matrix Dynamics and Fetal Membrane Rupture.,” *Reproductive Sciences (Thousand Oaks, Calif.)*, vol. 0, no. 0 (published online prior to print), Jan. 2012.

[5] V. Hampson, D. Liu, E. Billett, and S. Kirk, “Amniotic membrane collagen content and type distribution in women with preterm premature rupture of the membranes in pregnancy,” *British Journal of Obstetrics and Gynaecology*, vol. 104, pp. 1087-1091, Mar. 1997.

[6] V. Pandey et al., “The force required to rupture fetal membranes paradoxically increases with acute in vitro repeated stretching.,” *American Journal of Obstetrics and Gynecology*, vol. 196, no. 2, pp. 165.e1-7, Feb. 2007.

[7] S. Arikat et al., “Separation of amnion from choriodecidua is an integral event to the rupture of normal term fetal membranes and constitutes a significant component of the work required.,” *American Journal of Obstetrics and Gynecology*, vol. 194, pp. 211-7, Jan. 2006.

[8] M. Meinert et al., “Labour Induces Increased Concentrations of Biglycan and Hyaluronan in Human Fetal Membranes,” *Placenta*, vol. 28, pp. 482-6, 2007.

[9] A. Strohl et al., “Decreased adherence and spontaneous separation of fetal membrane layers--amnion and choriodecidua--a possible part of the normal weakening process.,” *Placenta*, vol. 31, pp. 18-24, Jan. 2010.

[10] G. Bourne, “The Foetal Membranes: A Review of the Anatomy of Normal Amnion and Chorion and Some Aspects of Their Function,” *Postgrad. Med. J.*, vol. 38, pp. 193-201, 1962.

[11] S. Parry and J. F. I. Strauss, “Mechanisms of Disease: Premature Rupture of the Fetal Membranes,” *The New England Journal of Medicine*, vol. 338, no. 10, pp. 663-670, Nov. 1998.

[12] M. Jabareen, A. S. Mallik, G. Bilic, A. H. Zisch, and E. Mazza, “Relation between mechanical properties and microstructure of human fetal membranes: an attempt towards a quantitative analysis.,” *European Journal of Obstetrics, Gynecology, and Reproductive Biology*, vol. 144, pp. S134-41, May 2009.

[13] J. T. Halaburt, N. Uldbjerg, R. Helmig, and K. Ohlsson, “The concentration of collagen and the collagenolytic activity in the amnion and the chorion.,” *European Journal of Obstetrics, Gynecology, and Reproductive Biology*, vol. 31, pp. 75-82, Apr. 1989.

[14] M. Meinert et al., “Proteoglycans and hyaluronan in human fetal membranes.,” *American Journal of Obstetrics and Gynecology*, vol. 184, no. 4, pp. 679-85, Mar. 2001.

[15] R. I. MacDermott and C. R. Landon, “The hydroxyproline content of amnion and prelabour rupture of the membranes.,” *European Journal of Obstetrics, Gynecology, and Reproductive Biology*, vol. 92, pp. 217-21, Oct. 2000.

[16] A. D. Hieber et al., “Detection of elastin in the human fetal membranes: proposed molecular basis for elasticity.,” *Placenta*, vol. 18, pp. 301-12, May 1997.

[17] S.-P. Wilshaw, J. N. Kearney, J. Fisher, and E. Ingham, “Production of an acellular amniotic membrane matrix for use in tissue engineering.,” *Tissue Engineering*, vol. 12, no. 8, pp. 2117-29, Aug. 2006.

[18] M. L. Oyen, S. E. Calvin, and D. V. Landers, “Premature rupture of the fetal membranes: Is the amnion the major determinant?,” *American Journal of Obstetrics and Gynecology*, vol. 195, no. 2, pp. 510-5, Aug. 2006.

[19] D. Kumar et al., “The effects of thrombin and cytokines upon the biomechanics and remodeling of isolated amnion membrane, in vitro.,” *Placenta*, vol. 32, no. 3, pp. 206-13, Mar. 2011.

[20] R. Helmig, H. Oxlund, L. K. Petersen, and N. Uldbjerg, “Different biomechanical properties of human fetal membranes obtained before and after delivery.,” *European Journal of Obstetrics, Gynecology, and Reproductive Biology*, vol. 48, no. 3, pp. 183-9, Mar. 1993.

[21] C. J. Lockwood et al., “Fetal Fibronectin in Cervical and Vaginal Secretions as a Predictor of Preterm Delivery,” *The New England Journal of Medicine*, vol. 325, no. 10, pp. 669-674, 1991.

[22] J. McLaren, D. J. Taylor, and S. C. Bell, “Increased concentration of pro-matrix metalloproteinase 9 in term fetal membranes overlying the cervix before labor: implications for membrane remodeling and rupture.,” *American Journal of Obstetrics and Gynecology*, vol. 182, no. 2, pp. 409-16, Feb. 2000.

[23] M. E. Khwad et al., “Fetal Membranes From Term Vaginal Deliveries Have a Zone of Weakness Exhibiting Characteristics of Apoptosis and Remodeling,” *Journal of the Society for Gynecologic Investigation*, vol. 13, no. 3, pp. 191-195, 2006.

[24] C. J. Connon et al., “The Biomechanics of Amnion Rupture: An X-ray Diffraction Study,” *PLoS one*, no. 11, p. e1147, Jan. 2007.

[25] M. Lappas et al., “MAPK and AP-1 proteins are increased in term pre-labour fetal membranes overlying the cervix: regulation of enzymes involved in the degradation of fetal membranes.,” *Placenta*, vol. 32, no. 12, pp. 1016-25, Dec. 2011.

[26] M. L. Oyen, R. F. Cook, and S. E. Calvin, “Mechanical failure of human fetal membrane tissues.,” *Journal of Materials Science. Materials in Medicine*, vol. 15, no. 6, pp. 651-8, Jun. 2004.

[27] W. K. Chua and M. L. Oyen, “Do we know the strength of the chorioamnion? A critical review and analysis.,” *European Journal of Obstetrics, Gynecology, and Reproductive Biology*, vol. 144, pp. S128-33, May 2009.

[28] G. Zegels, G. A. A. Van Raemdonck, E. P. Coen, W. A. A. Tjalma, and X. W. M. Van Ostade, “Comprehensive proteomic analysis of human cervical-vaginal fluid using colposcopy samples.,” *Proteome Science*, vol. 7, pp. 1-16, Jan. 2009.

[29] L. L. Klein, K. R. Jonscher, M. J. Heerwagen, R. S. Gibbs, and J. L. McManaman, “Shotgun proteomic analysis of vaginal fluid from women in late pregnancy.,” *Reproductive Sciences (Thousand Oaks, Calif.)*, vol. 15, no. 3, pp. 263-73, Apr. 2008.

[30] R. Pfundt et al., “Constitutive and inducible expression of SKALP/elafin provides anti-elastase defense in human epithelia.,” *The Journal of Clinical Investigation*, vol. 98, no. 6, pp. 1389-99, Sep. 1996.

[31] M. Fluckinger, H. Haas, P. Merschak, B. J. Glasgow, and B. Redl, “Human Tear Lipocalin Exhibits Antimicrobial Activity by Scavenging Microbial Siderophores,” *Antimicrobial Agents and Chemotherapy*, vol. 48, no. 9, pp. 3367-3372, 2004.

[32] G. T. Tsangaris et al., “The normal human amniotic fluid supernatant proteome.,” *In vivo (Athens, Greece)*, vol. 20, pp. 479-90, 2006.

[33] G. Tsangaris, R. Weitzdörfer, D. Pollak, G. Lubec, and M. Fountoulakis, “The amniotic fluid cell proteome.,” *Electrophoresis*, vol. 25, no. 6, pp. 1168-73, Mar. 2004.

[34] S.-J. Park et al., “Proteome analysis of human amnion and amniotic fluid by two-dimensional electrophoresis and matrix-assisted laser desorption/ionization time-of-flight mass spectrometry.,” *Proteomics*, vol. 6, pp. 349-63, Jan. 2006.

[35] A. Hopkinson, R. S. McIntosh, V. Shanmuganathan, P. J. Tighe, and H. S. Dua, “Proteomic analysis of amniotic membrane prepared for human transplantation: characterization of proteins and clinical implications.,” *Journal of proteome research*, vol. 5, pp. 2226-35, Sep. 2006.

[36] R. Romero, C. Avila, C. A. Brekus, and R. Morotti, “The Role of Systemic and Intrauterine Infection in Preterm Parturition,” *The Annals of the New York Academy of Sciences*, vol. 622, pp. 355-375, 1991.

[37] R. Romero, N. Kadar, J. C. Hobbins, and J. W. Duff, “Infection and labor: The detection of endotoxin in amniotic fluid,” *American Journal of Obstetrics and Gynecology*, vol. 157, no. 4, pp. 815-819, 1987.

[38] R. Romero, J. C. Hobbins, and M. D. Mitchell, “Endotoxin stimulates prostaglandin E2 production by human amnion,” *Obstetrics & Gynecology*, vol. 71, pp. 227-228, 1988.

[39] R. Romero et al., “Infection and Labor 4: Cachectin tumor necrosis factor in the amniotic fluid of women with intraamniotic infection and preterm labor,” *American Journal of Obstetrics and Gynecology*, vol. 161, no. 2, pp. 336-341, 1989.

[40] M. I. Evans, S. N. Hajj, D. Devoe, Lawrence, N. S. Angerman, and A. H. Moawad, “C-reactive protein with premature rupture of membranes and premature labor,” *American Journal of Obstetrics and Gynecology*, vol. 138, no. 6, pp. 648-652, 1980.

[41] C. Iavazzo et al., “The role of human beta defensins 2 and 3 in the second trimester amniotic fluid in predicting preterm labor and premature rupture of membranes.,” *Archives of Gynecology and Obstetrics*, vol. 281, no. 5, pp. 793-9, May 2010.

[42] W. G. Rice, T. Ganz, J. M. Kinkade, M. E. Selsted, R. I. Lehrer, and R. T. Parmley, “Defensin-rich dense granules of human neutrophils.,” *Blood*, vol. 70, no. 3, pp. 757-65, Sep. 1987.

[43] M. G. Gravett et al., “Diagnosis of Intra-amniotic Infection by Proteomic Profiling and Identification of Novel Biomarkers,” *JAMA*, vol. 292, no. 4, pp. 462-469, 2004.

[44] N. Athayde et al., “A role for matrix metalloproteinase-9 in spontaneous rupture of the fetal membranes.,” *American Journal of Obstetrics and Gynecology*, vol. 179, no. 5, pp. 1248-53, Nov. 1998.

[45] J. A. McGregor, J. I. French, D. Lawellin, A. Franco-Buff, C. Smith, and J. K. Todd, “Bacterial Protease-Induced Reduction of Chorioamniotic Membrane Strength and Elasticity,” *Obstetrics & Gynecology*, vol. 69, no. 2, pp. 167-74, 1987.

[46] P. Xu, N. Alfaidy, and J. R. G. Challis, “Expression of Matrix Metalloproteinase (MMP)-2 and MMP-9 in Human Placenta and Fetal Membranes in Relation to Preterm and Term Labor.,” *The Journal of Clinical Endocrinology and Metabolism*, vol. 87, no. 3, pp. 1353-61, Mar. 2002.

[47] D. Draper, J. Mcgregor, J. Hall, and W. Jones, “Elevated protease activities in human amnion and chorion correlate with preterm premature rupture of membranes,” *American Journal of Obstetrics and Gynecology*, vol. 173, no. 5, pp. 1506-1512, 1995.

[48] J. F. Woessner, “Matrix tissue metalloproteinases remodeling and their inhibitors in connective,” *The FASEB Journal*, vol. 5, pp. 2145-2154, 1991.

[49] F. Vadillo-Ortega, A. Hernandez, G. Gonzalez-Avila, L. Bermejo, I. Kazushi, and J. F. I. Strauss, “Increased matrix metalloproteinase activity and reduced tissue inhibitor of metalloproteinases-1 levels in amniotic fluids from pregnancies complicated by premature rupture of membranes,” *American Journal of Obstetrics and Gynecology*, vol. 174, no. 4, pp. 1371-1376, 1996.

[50] M. K. W. Di Quinzio et al., “Proteomic Analysis of Human Cervico-Vaginal Fluid Displays Differential Protein Expression in Association with Labor Onset at Term research articles,” *Journal of Proteome Research*, vol. 6, pp. 1916-1921, 2008.

[51] R. Romero et al., “The natural interleukin-1 receptor antagonist in term and preterm parturition,” *American Journal of Obstetrics and Gynecology*, vol. 167, no. 4, pp. 863-872, 1992.

[52] G. J. Kim et al., “Expression of bone morphogenetic protein 2 in normal spontaneous labor at term, preterm labor, and preterm premature rupture of membranes.,” *American Journal of Obstetrics and Gynecology*, vol. 193, no. 3 Pt 2, pp. 1137-43, Sep. 2005.

[53] R. H. Butt, M. W. Y. Lee, S. A. Pirshahid, P. S. Backlund, S. Wood, and J. R. Coorssen, “An Initial Proteomic Analysis of Human Preterm Labor : Placental Membranes research articles,” *Journal of proteome research*, vol. 5, pp. 3161 - 3172, 2006.

[54] D. C. Liebler, *Introduction to Proteomics: Tools for the New Biology*. Human Press Inc., 2002.

[55] H. Steen and M. Mann, “The ABC’s (and XYZ's) of peptide sequencing.,” *Nature Reviews, Molecular Cell Biology*, vol. 5, no. 9, pp. 699-711, Sep. 2004.

[56] C. Dass, “Ionization Methods,” in *Principles and Practice of Biological Mass Spectrometry*, 2001, pp. 11-58.

[57] R. B. Cole, “On the Mechanism of Electrospray Ioniation Mass Spectrometry,” in *Electrospray and MALDI Mass Spectrometry*, 2010, pp. 3-48.

[58] C. Dass, “Mass Analysis and Ion Detection,” in *Principles and Practice of Biological Mass Spectrometry*, 2001, pp. 59-94.

[59] C. Dass, “Tandem Mass Spectrometry,” in *Principles and Practice of Biological Mass Spectrometry*, 2001, pp. 95-115.

[60] R. Mattieson and K. E. Mutenda, “Introduction to Proteomics,” in *Mass Spectrometry Data Analysis in Proteomics*, R. Mattieson, Ed. Humana Press, 2007, pp. 1-35.

[61] A. I. Nesvizhskii, “Protein Identification by Tandem Mass Spectrometry and Sequence Database Searching,” in *Mass Spectrometry Data Analysis in Proteomics*, R. Matthieson, Ed. 2007, pp. 87-119.

[62] K. A. Neilson et al., “Less label, more free: approaches in label-free quantitative mass spectrometry.,” *Proteomics*, vol. 11, no. 4, pp. 535-53, Feb. 2011.

[63] B. Zhang, N. C. VerBerkmoes, M. A. Langston, E. Uberbacher, R. L. Hettich, and N. F. Samatova, “Detecting Differential and Correlated Protein Expression in Label-Free Shotgun Proteomics.,” *Journal of Proteome Research*, vol. 5, no. 11, pp. 2909-18, Nov. 2006.

[64] J. Lee, “Normalized Spectra Example", personal communication, July 8, 2011.

[65] D. W. Huang, B. T. Sherman, and R. a Lempicki, “Systematic and integrative analysis of large gene lists using DAVID bioinformatics resources.,” *Nature protocols*, vol. 4, no. 1, pp. 44-57, Jan. 2009.

[66] D. W. Huang, B. T. Sherman, and R. a Lempicki, “Bioinformatics enrichment tools: paths toward the comprehensive functional analysis of large gene lists.,” *Nucleic acids research*, vol. 37, no. 1, pp. 1-13, Jan. 2009.

[67] J. Woessner, J.F., “The Determination of Hydroxyproline in Tissue and Protein Samples Containing Small Proportions of this Imino Acid,” *Archives of Biochemistry and Biophysics*, vol. 93, pp. 440-447, 1961.

[68] “Uniprot Protein Knowledgebase,” *Uniprot Protein Knowledgebase*, 2011. [Online]. Available: www.uniprot.org. [Accessed: 01-Dec-2011].

[69] J. Nishihira, “Macrophage Migration Inhibitory Factor (MIF): Its Essential Role in the Immune System and Cell Growth,” *Journal of interferon & cytokine research : the official journal of the International Society for Interferon and Cytokine Research*, vol. 20, no. 9, pp. 751-62, Sep. 2000.

[70] M. J. Hardman, A. Waite, L. Zeef, M. Burow, T. Nakayama, and G. S. Ashcroft, “Macrophage migration inhibitory factor: a central regulator of wound healing.,” *American Journal of Pathology*, vol. 167, no. 6, pp. 1561-74, Dec. 2005.

[71] T. Chaiworapongsa et al., “Macrophage migration inhibitory factor in patients with preterm parturition and microbial invasion of the amniotic cavity.,” *The journal of maternal-fetal & neonatal medicine : the official journal of the European Association of Perinatal Medicine, the Federation of Asia and Oceania Perinatal Societies, the International Society of Perinatal Obstetricians*, vol. 18, no. 6, pp. 405-16, Dec. 2005.

[72] R. L. Caldwell, S. R. Opalenik, J. M. Davidson, M. Caprioli, and L. B. Nanney, “Tissue profiling MALDI mass spectrometry reveals prominent calcium-binding proteins in the proteome of regenerative MRL mouse wounds,” *Wound Repair Regen*, vol. 16, no. 3, pp. 442-449, 2008.

[73] G. Bilic et al., “Injectable candidate sealants for fetal membrane repair: bonding and toxicity in vitro.,” *American Journal of Obstetrics and Gynecology*, vol. 202, no. 1, pp. 85.e1-9, Jan. 2010.

[74] V. D. Jain and A. Sciscione, “Considerations in membrane resealing after preterm PROM.,” *Clinical Obstetrics and Gynecology*, vol. 54, no. 2, pp. 351-7, Jun. 2011.

[75] S. Barlage et al., “ApoE-containing high density lipoproteins and phospholipid transfer protein activity increase in patients with a systemic inflammatory response.,” *Journal of Lipid Research*, vol. 42, no. 2, pp. 281-90, Mar. 2001.

[76] K. Myers, S. Socrate, D. Tzeranis, and M. House, “Changes in the biochemical constituents and morphologic appearance of the human cervical stroma during pregnancy.,” *European Journal of Obstetrics, Gynecology, and Reproductive Biology*, vol. 144, pp. S82-9, May 2009.

[77] A. K. Williamson, A. C. Chen, K. Masuda, E. J.-M. a Thonar, and R. L. Sah, “Tensile mechanical properties of bovine articular cartilage: variations with growth and relationships to collagen network components.,” *Journal of Orthopaedic Research : official publication of the Orthopaedic Research Society*, vol. 21, no. 5, pp. 872-80, Sep. 2003.

[78] T. P. Prevost, “Biomechanics of the Human Chorioamnion,” M.S. thesis, Dept. of Materials Science and Engineering, Massachusetts Institute of Technology, 2006.

[79] R. L. Stevens, M. Colombo, J. J. Gonzales, W. Hollander, and K. Schmid, “The glycosaminoglycans of the human artery and their changes in atherosclerosis.,” *The Journal of Cinical Investigation*, vol. 58, no. 2, pp. 470-81, Aug. 1976.

[80] H. Oxlund, R. Helmig, J. T. Halaburt, and N. Uldbjerg, “Biomechanical analysis of human chorioamniotic membranes.,” *European Journal of Obstetrics, Gynecology, and Reproductive Bology*, vol. 34, no. 3, pp. 247-55, Mar. 1990.